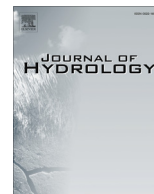




Contents lists available at ScienceDirect

Journal of Hydrology

journal homepage: www.elsevier.com/locate/jhydrol

Research papers

Estimation of stream-aquifer exchanges at regional scale using a distributed model: Sensitivity to in-stream water level fluctuations, riverbed elevation and roughness

Fulvia Baratelli^{a,*}, Nicolas Flipo^a, Florentina Moatar^b^a MINES ParisTech, PSL Research University, Geosciences Department, Fontainebleau, France^b Laboratoire GEHCO, UFR sciences et techniques, Université François Rabelais, Tours, France

ARTICLE INFO

Article history:

Received 4 November 2015

Received in revised form 6 September 2016

Accepted 16 September 2016

Available online xxxx

This manuscript was handled by K. Georgakakos, Editor-in-Chief, with the assistance of Jennifer Guohong Duan, Associate Editor

Keywords:

Surface-subsurface interactions

Modeling

Hydrology

Hydrogeology

Sensitivity analysis

Loire river basin

ABSTRACT

Several studies on stream-aquifer interactions focus on the local scale. However, the estimation of stream-aquifer exchanges for a regional river network remains challenging. This study aims at assessing the sensitivity of distributed stream-aquifer exchanges to in-stream water level fluctuations, riverbed elevation and Manning roughness coefficient.

An integrated distributed surface-subsurface model is applied to the Loire river basin (117,480 km², France), where in-stream water level fluctuations are taken into account with a simplified Manning-Strickler approach. The stream-aquifer exchanges are analyzed at pluri-annual and annual scales, as well as during short-term hydrological events.

The model simulates the spatio-temporal variability of in-stream water levels accurately, with Nash coefficients up to 0.96 for the Loire river. The river network mainly drains the aquifer system. The average net exchanged flow is $2 \cdot 10^{-2} \text{ m}^3 \text{ s}^{-1} \text{ km}^{-1}$, which corresponds to 12% of the averaged discharge at the outlet of the basin.

The assumption of constant river stages significantly impacts the total infiltration (–70%) and exfiltration (–10%) in the basin, whereas it has a negligible influence on the average net flux. The river fluctuations increase the time variability of the stream-aquifer exchanges and may determine flow reversals during flood events and also more frequently for river stretches at equilibrium with its nearby aquifer.

This study highlights the importance of accounting for river stage fluctuations in the modeling of regional hydrosystems. Moreover, a sensitivity analysis indicates that it is mandatory to develop new methodologies to better estimate the riverbed elevation at high resolution for a river network at regional scale. In a lesser extent, errors on Manning coefficient affect the timing of infiltration and exfiltration, leading to temporally localized discrepancies. However it does not affect the estimates of the global net exchanges significantly.

© 2016 Elsevier B.V. All rights reserved.

1. Introduction

The concept of hydrosystem (see, e.g., Dooge (1968), Kurtulus et al. (2011), Flipo et al. (2014)) reflects the need to consider the interactions between the different components of the water cycle in order to evaluate the water and solute fluxes properly. In particular, the stream-aquifer interface controls the interactions between surface water and groundwater. The evaluation of the water fluxes at this interface is then a primary task to correctly simulate the hydrosystem functioning (Fleckenstein et al., 2010; Saleh et al., 2011; Flipo et al., 2014) and predict its response to

climatic and anthropogenic stresses (Scibek and Allen, 2006; Scibek et al., 2007; Zume and Tarhule, 2008; Zume and Tarhule, 2011; Waibel et al., 2013; Graham et al., 2015).

Stream-aquifer interfaces can be described at different scales (Flipo et al., 2014): local (10 cm to 10 m), intermediate or reach (10 m to 1 km), watershed (10–1000 km²), regional (10,000 km² to 1 M km²) and continental (>10 M km²). The regional scale is of utmost importance since environmental regulatory frameworks, such as the European Water Framework Directive (EU Parliament, 2008), and water resource management plans (Pryet et al., 2015) are often set at this scale.

In their extensive literature review, Flipo et al. (2014) pointed out that, among 183 publications concerning the usage of distributed physically based hydrological-hydrogeological models,

* Corresponding author.

E-mail address: fulvia.baratelli@mines-paristech.fr (F. Baratelli).

only 19 pertain to the regional scale. Except for [Monteil \(2011\)](#) and [Pryet et al. \(2015\)](#), none of these publications explicitly perform a distributed quantification of the stream-aquifer exchanges. Further work is then needed to improve the modeling of the stream-aquifer exchanges at the regional scale. The classical approach is a conductance model ([Rushton and Tomlinson, 1979](#)) assuming constant river stages over time. To the authors' knowledge, the only study taking into account water level fluctuations at the regional scale was carried out by [Pryet et al. \(2015\)](#).

Nevertheless, the effect of water level fluctuations on stream-aquifer exchanges was studied by a few authors at intermediate and watershed scale. At the intermediate scale, in-stream water level fluctuations may determine temporary reversals of the gaining or losing regime for some river reaches, particularly during flood events ([Cloutier et al., 2014](#)). Such reversals could have a major influence on the fluxes of contaminants ([Zachara et al., 2013](#); [Batlle-Aguilar et al., 2014](#)). An accurate description of the river longitudinal water level distribution is also important to estimate groundwater residence times, as shown at reach scale by [Diem et al. \(2014\)](#).

At the watershed scale, in-stream water level fluctuations have a significant impact on the stream-aquifer exchanges and on the near-river piezometric head distribution ([Saleh et al., 2011](#)). Moreover, in-stream water level fluctuations slightly increase both the global exfiltration and the global infiltration in the basin, with a resulting negligible variation of the net stream-aquifer exchange ([Saleh et al., 2011](#)). At larger scales (regional or continental), the assessment of the impact of in-stream water level fluctuations on the stream-aquifer exchanges still needs to be developed.

The approach to account for river stage fluctuations in coupled hydrological-hydrogeological models depends on the scale of the modeled domain as well as on data availability. At the watershed scale, the methodology is generally based on the availability of river cross-section profiles. This is the case of the study published recently by [Foster and Allen \(2015\)](#) concerning a mountain to coast 930 km²-watershed. The net and absolute fluxes were estimated taking into account the in-stream water level fluctuations by means of the diffusive wave approximation of the one-dimensional Saint-Venant equations.

In [Saleh et al. \(2011\)](#), a one-dimensional Saint-Venant model is employed to derive the rating curves to be used in the hydrogeological model to compute the water stages from the simulated discharge. This approach is successful to accurately simulate river stage variability and near-river piezometric head distribution with a rather low computational cost, as the hydraulic model is not coupled to the hydrogeological model, but it is used to construct the rating curves. However, this method is also based on the availability of surveyed cross-section, which is often not guaranteed for regional scale basins.

At the regional scale, [Pryet et al. \(2015\)](#) simulate in-stream water level fluctuations with a simplified Manning-Strickler approach, which requires as input data some basic morphological features (river width, riverbed elevation and longitudinal slope) as well as the Manning roughness coefficient. The geomorphological properties are estimated with a Digital Elevation Model (DEM), while the roughness coefficient is calibrated against observed discharge and river stages as in [Saleh et al. \(2011\)](#). This is an acceptable compromise for simulating river stages at the regional scale ([Saleh et al., 2013](#)).

The approach followed by [Pryet et al. \(2015\)](#) is suitable for regional hydrosystems where surveyed cross-sections are not available. However, the river network morphological parameters are difficult to estimate at the regional scale and the values derived from a DEM may be affected by significant errors. The question then arises whether such errors in the modeling of river stage

variability may hinder a correct evaluation of the stream-aquifer exchanges.

In this context, the present work aims at answering two main questions. First of all, which are the effects of in-stream water level fluctuations on the stream-aquifer exchanges for a regional hydrosystem? The answer to this question has a practical application for hydrosystem modeling because it will determine whether a simpler model assuming constant river stages is reliable or not.

The second question is: which are the effects of the uncertainties related to the modeling of in-stream water level fluctuations on the stream-aquifer exchanges? In other words, does the answer to the first question depend on the uncertainties on input quantities like the DEM and the Manning roughness coefficient?

In order to address these questions, an integrated distributed surface-subsurface model, Eau-Dyssée ([Flipo et al., 2012](#); [Flipo, 2013](#)), is applied to the Loire river basin (117,480 km²), where the variability of in-stream water levels is taken into account following the approach of [Pryet et al. \(2015\)](#). The effects of river stage fluctuations on the stream-aquifer exchanges are assessed by performing a simulation with constant river stages. Moreover, a sensitivity analysis of the stream-aquifer exchanges on some of the parameters controlling the river stage variability, namely, the DEM, which is used to estimate the riverbed elevation, and the Manning coefficient, is performed.

2. The Eau-Dyssée platform for hydrosystem modeling

Eau-Dyssée is a distributed model that allows the simulation of the different components of the water cycle in a hydrosystem. Detailed descriptions of the model can be found in [Flipo \(2013\)](#), [Flipo et al. \(2012\)](#), [Saleh et al. \(2011\)](#) and [Saleh \(2010\)](#). Here, only the main features are briefly recalled.

Eau-Dyssée conceptually divides a hydrosystem into three interacting compartments: surface, unsaturated zone and saturated zone. Specifically, the model couples six modules which simulate the surface water mass balance, the runoff, the river flow, the in-stream water level fluctuations, the flow in the unsaturated zone, the flow in the saturated zone ([Fig. 1](#)).

The surface water balance module is a conceptual model that computes runoff, real evapotranspiration, soil storage and infiltration from the input data of precipitations and potential evapotranspiration. This model integrates information on land use and soil cover through a seven-parameter conceptual model (production function, [Deschesnes et al. \(1985\)](#)).

The surface runoff is routed to the river network by the ISO module, according to which the runoff reaches the river network with a delay that depends on topography and concentration time ([Flipo et al., 2012](#)).

Water reaching the river network is routed by the module RAPID (Routing Application for Parallel Computation of Discharge, see [David et al. \(2011a,b, 2013\)](#)), which is based on a one-dimensional Muskingum scheme.

Then, the QTOZ module ([Saleh et al., 2011](#); [Saleh, 2010](#)) calculates the in-stream water level as a function of the discharge routed by the module RAPID. The module allows three options: fixed water levels, water levels estimated from a rating curve or water levels estimated using the Manning-Strickler equation.

Infiltrated water flows through the unsaturated zone before reaching the saturated zone. This is simulated in the conceptual model NONSAT by introducing a succession of reservoirs, whose number increases with the thickness of the unsaturated zone. This simplified description of the unsaturated zone simulates the delay between water infiltration and flow in the saturated zone.

The flow in the saturated zone is simulated by the module SAM, which is a physically-based distributed hydrogeological model for

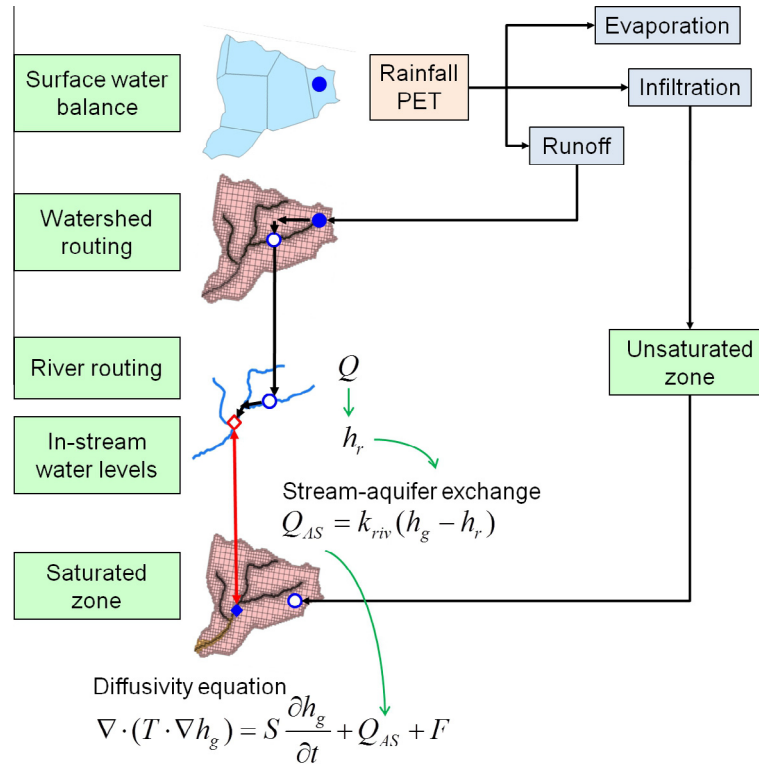


Fig. 1. Conceptual scheme of coupled surface-subsurface model Eau-Dyssée. Q is river discharge, h_r the river stage elevation, Q_{AS} the stream-aquifer exchange, k_{riv} the conductance, h_g the groundwater head, T the transmissivity, S the storage coefficient and F the source term. Adapted from Flipo et al. (2012).

multi-layer aquifer systems initially developed by Ledoux (1975), de Marsily et al. (1978) and Levassor and Ledoux (1996). This model solves the diffusivity equation (de Marsily, 1986) with a quasi-3D finite-differences scheme: the flow is assumed to be horizontal in each layer, whereas the aquitards between the layers are characterized by vertical flow. The SAM module is coupled to the surface modules (RAPID and QTOZ) through the stream-aquifer exchanges (Fig. 1).

2.1. Estimation of stream-aquifer exchanges

In regional surface water-groundwater models, the river width is generally smaller than the mesh size of the model. As a consequence, it is not meaningful to set the continuity of the water level in the cells representing the stream-aquifer interface. In this case, the stream-aquifer exchanges are commonly estimated with a conductance model, according to which the water flux between aquifer and stream, Q_{AS} [$\text{m}^3 \text{s}^{-1}$], is proportional to the difference between the piezometric head, h_g [m], and the in-stream water level, h_r [m], i.e.:

$$Q_{AS}(\mathbf{x}, t) = k_{riv}(\mathbf{x}) [h_g(\mathbf{x}, t) - h_r(\mathbf{x}, t)], \quad (1)$$

where the proportionality constant k_{riv} [$\text{m}^2 \text{s}^{-1}$] is the conductance of the stream-aquifer interface, \mathbf{x} is the location and t is time. According to Eq. (1), the flux at the interface is positive if the piezometric head is greater than the river water level, that is, the aquifer exfiltrates to the river, which is in a gaining regime. On the contrary, Q_{AS} is negative if $h_g < h_r$, that is, the river is in a losing regime and it infiltrates towards the aquifer.

Although the conductance coefficient is traditionally estimated from the properties of the riverbed deposits, Rushton (2007) showed that the main factor controlling the conductance coefficient is the horizontal hydraulic conductivity k_H [m s^{-1}] of the underlying aquifer, according to the following expression:

$$k_{riv} = f k_H L, \quad (2)$$

where f is an adjustable correction factor, generally ranging between 0.9 and 1.2 (Rushton, 2007), and L [m] is the model mesh size. This approach was followed by Pryet et al. (2015) to estimate the stream-aquifer exchanges in the Seine river basin (65,000 km^2), after calibrating the correction factor f .

In order to simulate the possible disconnection between streams and aquifers, the Eau-Dyssée model limits the infiltration rate to a maximum value, Q_{lim} (Saleh et al., 2011; Flipo et al., 2014), which represents the infiltration occurring by gravity in a disconnected system (Brunner et al., 2009; Rivi re et al., 2014; Xie et al., 2014). For regional temperate hydrosystems, Q_{lim} also plays a role in case of floods, as discussed later in Section 5.3.2.

2.2. In-stream water level fluctuations

The Manning-Strickler equation allows the calculation of the average fluid velocity v [m s^{-1}] for uniform flow in open channels (Chow, 1959):

$$v = n^{-1} R^{2/3} S^{1/2}, \quad (3)$$

where n is the Manning roughness coefficient [$\text{s m}^{-1/3}$], R is the hydraulic radius [m], and S [–] is the slope of the energy line which, given the hypothesis of uniform flow, can be considered equal to the slope of the riverbed. If A [m^2] is the area of the wetted surface, Eq. (3) can be rewritten in terms of the discharge $Q = vA$:

$$Q(t) = n^{-1} R^{2/3} S^{1/2} A. \quad (4)$$

If it is assumed that the river section is rectangular and that its width, W [m], is much greater than its depth, d [m], then $A = Wd$ and $R \approx d$. Consequently, Eq. (4) can be rewritten, in terms of d , as:

$$d(t) = \left(\frac{Q(t)n(t)}{W(t)S(t)^{1/2}} \right)^{3/5}, \quad (5)$$

where the dependence on time t has been explicitly indicated and $Q(t)$ is computed by the river routing module (Fig. 1). As a first approximation, n , W and S are assumed to be constant. In-stream water levels, h_r [m], can then be computed as

$$h_r(t) = b + d(t), \quad (6)$$

where b [m] is the riverbed elevation and d is given by Eq. (5).

3. Implementation of the Loire river basin model

3.1. The Loire basin

The Loire river basin (117,480 km²) is the largest basin entirely located in France and it covers one fifth of the country (Fig. 2).

The climatic regime of the Loire basin is pluvial. The average precipitation over the period 1970–2009 ranges from more than 1000 mm/a in the upstream part of the basin to less than 700 mm/a in the downstream plains, whereas the average precipitation for the entire basin is 815 mm/a. The interannual variability is significant, as the annual averages can vary from 450 mm/a in a dry year like 1975–1976 to 970 mm/a in a humid year like 2000–2001.

Concerning the hydrology of the basin, the Loire river is 1013 km long and it is characterized by a pluvial hydrological regime, with a high river flow period in winter and a low-flow period in summer. A periodicity of 17 years, associated with the North Atlantic Oscillation (NAO), has been observed in climatic variables and stream discharge (Massei et al., 2010), as well as in groundwater levels (Flipo et al., 2012). The mean daily discharge at the outlet of the basin (Saint-Nazaire, see Fig. 2) is 883 m³ s⁻¹ over the 17-years period 1998–2015. The hydrological regime is very irregular

due to intense floods and droughts. For example, the mean daily discharge at Saint-Nazaire is 130 m³ s⁻¹ for the 5-year droughts and 5100 m³ s⁻¹ for the 20-year floods.

The central part of the basin is composed of multi-layer sedimentary formations, whereas the remainder of the basin lies on crystalline formations. In the central basin the main aquifer units are the Oligocene-Eocene (Beauce), the Upper Cretaceous chalk and the Cenomanian sands. Local karst formations are identified around the town of Orléans (Fig. 2): in particular, the Loire river loses water in the karst system between Châteauneuf and Jargeau (Fig. 2), upstream of Orléans, and then it regains this water through the Loiret river (Fig. 2) downstream of Orléans (Chery, 1983).

3.2. Domain, boundary conditions and discretization

The present paper is based on the coupled hydrological/hydrogeological model of the Loire river basin developed by Monteil (2011). In this work, the modeled domain is represented by the part of the basin downstream of the confluence between the Loire and the Allier rivers, i.e., downstream of the Cours-les-Barres gauging station (Fig. 2), where the observed discharge is imposed as a model boundary condition. This choice simplifies the model construction, as three dams are present on the Loire river upstream of the Cours-les-Barres gauging station. The modeled area includes the part of the neighboring Seine river basin which overlays the Beauce aquifer, in order to take into account the time variability of the piezometric crest between the two hydrogeological basins. The area of the modeled domain is 90,000 km², of which 38,700 km² are characterized by the presence of outcropping aquifers interacting with the stream network.

Three aquifers are modeled, namely, from top to bottom, the Oligocene-Eocene (Beauce), the Upper Cretaceous chalk and the Cenomanian sands, which are separated from the underlying Albian aquifer by the low-permeability Gault clayed aquitard. A fixed-head boundary condition is imposed along the Seine river,

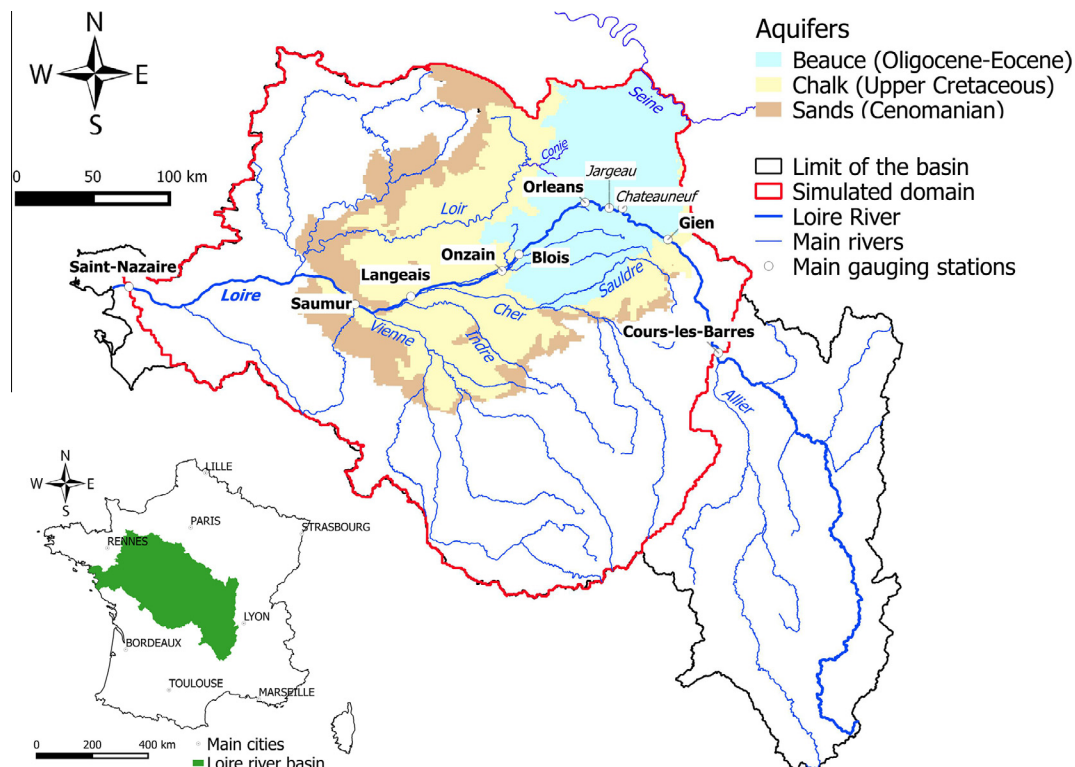


Fig. 2. The Loire river basin.

whereas a no-flow boundary condition is imposed at the remaining aquifer borders, as well as at the bottom of the deepest aquifer, i.e., the Cenomanian sands.

The hydrological mass balance is computed on 90 units, called production cells, which result from the intersection of two data sets: the Corine Land Cover data set defining the land use in France (<http://www.eea.europa.eu>) and the INRA Soil database defining the classification of soil geologic types in France (King et al., 1995). The production cells are characterized by different combinations of 22 production functions, each of which is defined by seven parameters governing the balance between infiltrated water, evapotranspiration and runoff.

The stream network is obtained from a Digital Elevation Model (DEM) resampled on square cells of side 1 km with the HydroDem software (Leblais, 2008). Only the cells draining more than 50 km² are retained, leading to 16,141 river cells, of which 5244 are connected with an underlying aquifer. The surface is discretized in 63,234 nested square cells whose size ranges from 1 km to 8 km. The unsaturated zone is represented by a number of reservoirs proportional to its thickness. The three aquifer units were discretized with a total of 37,620 square cells with the same range of sizes as the surface cells.

3.3. Input data

The model input data can be classified in forcings, observed time series of the hydrological and hydrogeological quantities (discharge, piezometric head and river stage) and calibration parameters.

The model forcings are represented by the meteorological inputs, i.e., precipitation and potential evapotranspiration, which are given by the Météo-France SAFRAN database at a 8 × 8 km² resolution and a daily time step (Quintana-Seguí et al., 2008). The basin is also characterized by the presence of several pumping sites for irrigation, drinking water supply and industrial needs. Information on the localization and the intensity of such water withdrawals are provided by the Water Agencies and are integrated in the model (Monteil, 2011).

The Banque Hydro database (www.hydro.eaufrance.fr) provides discharge and water stage time series at 161 gauging stations in the modeled domain. In the same region, the ADES database (www.ades.eaufrance.fr) provides piezometric head time series at 195 piezometers: 89 in the Beauce aquifer, 48 in the Upper cretaceous chalk aquifer and 58 in the Cenomanian sands aquifer. These observed time series are needed to calibrate and validate the model. Moreover, the discharge observed at the Cours-les-Barres gauging station and the water stages in the Seine river are also used as boundary conditions, as previously discussed.

The total number of calibration parameters of the Loire basin model developed by Monteil (2011) is 174,654; the reader is referred to that work and to Flipo et al. (2012) for a detailed description of such parameters.

A DEM is also required to define the topographic threshold for groundwater seepage, to simulate the watershed and river routing and, finally, to estimate the river stages, as detailed in Section 3.4.

3.4. Input data to simulate the time fluctuations of in-stream water levels

The simulation of variable river stages with the approach described in Section 2.2 requires the Manning coefficient n , which is calibrated as described in Section 3.5, as well as some morphological parameters (river width, riverbed elevation and slope). Measured cross-sections were available for the Loire river only, so that different methods had to be employed to estimate these

quantities for the remaining of the river network, as detailed in the following paragraphs.

3.4.1. River width

The bankfull width of the Loire river was approximated as the active-channel width, which was estimated by measuring the non-vegetated river width every 500 m on aerial photographs (Latapie et al., 2014). For the lower Strahler orders (Strahler, 1957) of the stream network, the values of river width were taken from the database SYRAH (Valette and Cunillera, 2010), which is also based on aerial photographs. The resulting river widths range from 2 m for the upstream tributaries to 530 m for the Loire river where it leaves the aquifer zone.

3.4.2. Riverbed elevation

The longitudinal distribution of the riverbed elevation along the Loire river was defined using the transversal profiles measured at 255 cross-sections, which have an average spacing of 1.6 km (Latapie et al., 2014). For each section, the 20% quantile of riverbed elevations was computed and assigned as riverbed elevation to the model cell containing that section. A linear interpolation was finally performed between the different sections in order to obtain the riverbed elevation for all the Loire river cells.

For the other streams of the Loire river network, the estimate of the riverbed elevation is based on the Manning-Strickler Eq. (6). In particular, if it is assumed that Eq. (6) holds in bankfull conditions, then the riverbed elevation can be computed as:

$$b = h_r^{bf} - \left(\frac{nQ^{bf}}{WS^{1/2}} \right)^{3/5}, \quad (7)$$

where h_r^{bf} and Q^{bf} denote the bankfull stage and discharge, respectively. h_r^{bf} is approximated by the DEM. Q^{bf} corresponds to an average return period of 1.5 years (Dunne and Leopold, 1978). Therefore, Q^{bf} was estimated for each river cell as the 75% quantile of the discharge distribution given by a pluri-annual simulation, for which the river stages are forced to be constant and equal to the bankfull stage.

3.4.3. Digital elevation model

The DEM used in this paper is given by the database ALTI at 25 m resolution (IGN, 2015). The bankfull stage is assigned to each river cell with a GIS treatment, by taking the minimum elevation among the 25 m pixels of the DEM that intersect that river cell. The drawback of this method is that the model (DEM-derived) river network does not perfectly overlap the real river network, so that the water surface in the stream network often shows a discontinuous downstream slope, which is physically inconsistent.

The algorithm described by Yamazaki et al. (2012), which was originally proposed by Soille (2004), was then used to correct the DEM in order to obtain a continuous downstream slope along the drainage network. This algorithm minimizes the modifications of the original DEM by combining the filling and carving approaches (Käser et al., 2013) and optimizing a function that defines the cost of the total modifications.

The resulting DEM is used to compute the reference riverbed elevation by subtracting the river depth following Eq. (7).

In order to analyze the model sensitivity to the riverbed elevation estimated using different DEM products, a second distribution of riverbed elevations is obtained from a coarser model, the SRTM3 (Farr et al., 2007), which is generated by radar interferometry and has a resolution of three arc-seconds, i.e., about 90 m. The distribution of the differences between the riverbed elevations computed with the SRTM3 and those computed with the DEM at 25 m resolution is characterized by an average value of −1.2 m and a

standard deviation of 2 m. The riverbed elevation remains unchanged for 15% of the river network, whereas it decreases for 66% and increases for 19% of the network. It could have been expected that a DEM with a smaller resolution leads to higher values of the riverbed elevation, as the larger size of the pixels implies a larger influence of the banks. This is not the case here. It can be explained by the fact that the two DEMs have not only a different resolution, but they also have been obtained with different techniques, radar interferometry for the SRTM3 and LIDAR for the DEM at 25 m.

3.4.4. Riverbed slope

For the Loire river, the riverbed longitudinal slope was computed from the riverbed elevation values, while for the remaining of the river network the slope was provided by the database SYRAH, where it is calculated from a DEM at 50 m resolution (Valette and Cunillera, 2010).

3.5. Calibration method

The coupled hydrological-hydrogeological model of the Loire basin was first calibrated by assuming constant in-stream water levels according to the stepwise procedure described in Monteil (2011) and Flipo et al. (2012). First a pre-calibration of the parameters of the production functions against the observed discharge is achieved to obtain a first estimate of the aquifer recharge. Then a calibration of the Beauce aquifer is performed with a hybrid method coupling manual and automatic calibration, the latter being performed with the successive flux estimation technique (Ponzini and Lozej, 1982; Pasquier and Marcotte, 2006; Flipo et al., 2012). Finally the calibration of the multi-layer aquifer system, which is iteratively conducted with the re-calibration of the surface parameters, is performed to take into account the interactions between surface water and groundwater. The model was calibrated over the period 1998–2008 and validated over the period 1974–1984. Moreover, a test simulation was performed over the 35 years period 1974–2009 (Monteil, 2011) to ensure the robustness of the parameter set as recommended by Flipo et al. (2012).

The riverbed conductance k_{riv} was considered by Monteil (2011) as a calibration parameter, whereas k_{riv} is computed here as in Pryet et al. (2015) according to Eq. (2), which requires the calibration of the correction factor f only. As shown by Rushton (2007), this coefficient is generally between 0.9 and 1.2, so that its calibration requires the exploration of a much narrower range than the calibration of k_{riv} . The calibration of f is performed by comparing the results of 8 simulations run with values of f ranging from 0.9 to 1.4, with a spacing of 0.1. The Nash-Sutcliffe efficiency coefficient (Nash and Sutcliffe, 1970), the absolute and relative bias and the Root Mean Square Error (RMSE) are calculated for each simulation at 161 discharge gauging stations and 195 piezometer locations in order to assess the model performances in terms of river discharge, piezometric head and in-stream water level.

The value of the maximum infiltration rate, Q_{lim} , is assumed to be uniform and equal to $0.1 \text{ m}^3 \text{ s}^{-1}$, according to the results of the calibration performed by Monteil (2011). The same value was obtained for the Oise river basin, a sub-basin of the Seine river basin (Saleh et al., 2011).

The simulation of the time variability of in-stream water levels requires the calibration of the Manning coefficient n for the 5244 river cells connected to an underlying aquifer. The Manning coefficient is related to the friction between the riverbed and the water flow. This coefficient depends on several factors: the roughness of the river bottom, the presence and type of vegetation on the banks, the irregularity of cross sections, the value of discharge and river stage (Chow, 1959). As it is difficult to have enough information

about all these factors for an entire river network, a first estimate of the Manning coefficient has been defined based on the stream Strahler order (see Table 1). In fact, this coefficient is generally smaller for rivers characterized by a smooth bottom, which is generally the case for the downstream rivers of the network.

The availability of river stage observations in the network permits to better estimate the Manning coefficient. In particular, Eqs. (6) and (5) allow the calculation of a time-dependent Manning coefficient:

$$n(t) = \frac{WS^{1/2} (h_r^{obs}(t) - b)^{5/3}}{Q^{obs}(t)}. \quad (8)$$

The average of $n(t)$ over the simulation period, which is denoted as \bar{n} , is used as the value of n to be inserted in Eq. (5). Assuming that the simulated discharge is a good approximation of the observed discharge, which is confirmed by the results of Monteil (2011), this method minimizes the difference between the simulated and observed river stages. This procedure is tested for the Loire river, where 6 gauging stations are available. The Manning coefficient is optimized station by station. The river is then divided in reaches of uniform n around each station.

3.6. Simulation scenarios

Five simulations are analyzed in this paper. The first simulation, referred to as the reference simulation, uses the reference parameters issued from the model calibration. A second simulation is performed by assuming constant in-stream water levels, with the objective of evaluating the effects of in-stream water level fluctuations on the stream-aquifer exchanges. In this case, the DEM is assumed to be an estimate of the average river stage. In the third simulation the SRTM3 DEM is employed to estimate the bankfull stage and then the riverbed elevation according to Eq. (7). Finally, two simulations were performed by changing the Manning coefficient all along the stream network by +20% and –20%, respectively, of the reference values.

For each simulation, the analysis of the stream-aquifer exchanges is performed both at the pluri-annual and annual time scales, as in Pryet et al. (2015). Moreover, the stream-aquifer exchanges are also analyzed at the scale of short-term hydrological events, when flow reversals can occur.

These different time scales are analyzed through five simulation scenarios. The pluri-annual scenario covers a period of 17 years (1990–2007), which is the duration of the cycle associated with the North Atlantic Oscillation (NAO) (Massey et al., 2010; Flipo et al., 2012). Due to the 17 years periodicity of the hydrological variability, this is the minimal period of time for calculating relevant pluri-annual averages. Two annual scenarios, denoted as WY and DY, were then defined as hydrological years characterized by wet and dry conditions, respectively. Finally, two short-term scenarios were defined as a single day of high-flow (HF) and low-flow (LF) conditions.

Table 1
Correspondence assumed between the Manning coefficient n and the Strahler order for the affluents of the Loire river.

Strahler	$n [\text{s m}^{-1/3}]$
1	0.067
2	0.050
3	0.040
4	0.033
5	0.029
≥6	0.025

The wet and dry years, as well as the high-flow and low-flow days, were selected according to the discharge time series at the outlet station of Saint-Nazaire: the wet year is 2000–2001 ($1553 \text{ m}^3 \text{ s}^{-1}$) and the dry year is 2005–2006 ($608 \text{ m}^3 \text{ s}^{-1}$), whereas the high-flow corresponds to 28/01/1995 ($6080 \text{ m}^3 \text{ s}^{-1}$) and the low-flow to 11/09/1996 ($124 \text{ m}^3 \text{ s}^{-1}$).

3.7. Quantification of the net and absolute stream-aquifer fluxes at the regional scale

The stream-aquifer exchanges are calculated according to Eq. (1) at each river network cell, i.e., at a 1 km resolution with a daily time step. In order to characterize the stream-aquifer exchanges at the regional scale, the quantities Q_{net} , $Q_{A \rightarrow S}$, $Q_{S \rightarrow A}$, $L_{A \rightarrow S}$ and $L_{S \rightarrow A}$ are computed. Q_{net} denotes the time average of the total net stream-aquifer flows for the whole river network. Similarly, $Q_{A \rightarrow S}$ (aquifer to stream flow) and $Q_{S \rightarrow A}$ (stream to aquifer flow) denote the absolute fluxes, respectively, exfiltrating and infiltrating. Moreover, $L_{A \rightarrow S}$ and $L_{S \rightarrow A}$ represent the percentages of the network length which are characterized by an average gaining or losing regime over the simulation period. Finally, L_0 is the percentage of the network length which is characterized by a negligible exchanged flux, i.e., with an absolute value less than $1 \text{ L s}^{-1} \text{ km}^{-1}$.

4. Results

4.1. Model performance

The water stage time variability along the Loire river is simulated with very good accuracy. The average Nash coefficient is 0.93, the average RMSE is 0.2 m and the bias ranges from -0.14 m to 0.23 m (Table 2 and Fig. 3c and d). Both the amplitude and the phase of the water level variations during an hydrological year are well described at all the gauging stations of the Loire river, and especially at the Blois station (Fig. 2c), which is located at the border between the Beauce aquifer and the outcropping of the Chalk aquifer, and at the Saumur station (Fig. 2d) which is located 30 km upstream the outlet of the aquifer zone. In other words, the regional model is able to represent the water level fluctuations during the high-flow and low-flow periods at the scale of the single gauging stations. To the authors' knowledge, no other publications reported such performances for water stages at the regional scale.

Less surprisingly, the model also reproduces with good accuracy the dynamics of the hydrographs: the average Nash coefficient over the whole simulation period is 0.96 at the outlet station of Saint-Nazaire (Table 3). The average Nash coefficient is 0.96 along the Loire river and 0.65 in the entire domain (Table 3). 89% of the discharge stations have Nash coefficients greater than 0.5 (Fig. 4).

Concerning the piezometric head, the average RMSE over the whole simulation period is 2.84 m for the Oligocene-Eocene aquifer, 5.22 m for the Upper Cretaceous chalk aquifer and 5.30 m for the Cenomanian sands aquifer. The average RMSE is smaller than 5 m for 80% of the piezometers in the domain (Fig. 5). These performances are satisfactory at the regional scale and correspond to

state-of-the-art model performances (Flipo, 2013; Pryet et al., 2015) (see Table 4).

4.2. Optimal parameters

The model performances are nearly insensitive to the value of the correction factor f of the riverbed conductance. In fact, the RMSE for the piezometric head only increases of 0.02 m when passing from $f = 0.9$ to $f = 1.4$, while the discharge at the Saumur station does not change with f . However, the best criteria are attained with the simulation using $f = 0.9$. This simulation has then been selected as the reference simulation.

Concerning the optimization of the Manning coefficient along the Loire river, the values of \bar{n} obtained as time average of the results of Eq. (8), as well as the corresponding RMSE for each station, are shown in Table 5. The Strahler order of the modeled Loire river is greater than 6, so that, according to Table 1, a uniform value $n = 0.025 \text{ s m}^{-1/3}$ should be applied. The RMSE corresponding to this situation is also shown in Table 5. It can be noticed that the values \bar{n} , calibrated station by station, do not always minimize the RMSE. In fact, the Manning coefficient computed by Eq. (8) changes with time, with lower values during low-flow periods and higher values during high-flow periods. Therefore, the choice of averaging $n(t)$ does not always lead to the minimum RMSE. In the reference simulation, the value n_0 assigned to each station is the one that minimizes the RMSE (Table 5). The resulting coefficients for the stations of Blois ($n_0 = 0.016 \text{ s m}^{-1/3}$) and Gien ($n_0 = 0.015 \text{ s m}^{-1/3}$) are lower than the range $0.025\text{--}0.1 \text{ s m}^{-1/3}$ expected for a natural river (Chow, 1959). As the Loire can be considered a natural river (no dredging nor channeling), this result could be explained by the fact that the Manning coefficient tends to compensate for the inaccuracy of the morphological parameters of Eq. (8), namely, river width, riverbed elevation and slope.

4.3. Reference spatial distribution of stream-aquifer exchanges

In the pluri-annual scenario, the river network mainly drains the aquifer system. Local re-infiltrations driven by large-scale structural heterogeneities are also observed. This configuration, which is typical of temperate continental hydrosystems (Flipo et al., 2014), is characterized by a variability at shorter time scales, during wet and dry hydrological years, as well as during short-term hydrological events (floods and droughts).

4.3.1. Pluri-annual configuration

The Loire river exchanges mainly with the Beauce aquifer, whereas the remaining of the stream network exchanges mainly with the Chalk and Cenomanian aquifers (Fig. 6), which are less permeable than the Beauce aquifer (Monteil, 2011; Flipo et al., 2012).

In particular, the area around Orléans is very active in terms of stream-aquifer exchanges (Fig. 6). Upstream Orléans, localized infiltration areas are present, where the average infiltration reaches the limit of $0.1 \text{ m}^3 \text{ s}^{-1} \text{ km}^{-1}$. Moreover, an exfiltration peak of nearly $1.9 \text{ m}^3 \text{ s}^{-1} \text{ km}^{-1}$ is observed about 30 km upstream Orléans, where localized karst systems were identified (Chery, 1983). The model does not explicitly take into account the karst systems. However, its calibration led to sharp contrasts of transmissivities in order to account for the effect of the karst on the local piezometric head distribution. This is the reason why a spatial alteration from infiltration to a high but narrow exfiltration peak is observed (Fig. 6). Downstream Orléans, an exfiltration peak, with flows up to $1.2 \text{ m}^3 \text{ s}^{-1} \text{ km}^{-1}$, is observed. This exfiltration zone was confirmed by means of an heat budget method (Moatar and Gailhard, 2006) based on river temperature estimated with satellite thermal infrared images (Lalot et al., 2015). A lower exfiltration

Table 2

Performance of the reference simulation in terms of in-stream water levels of the Loire river: statistical criteria over the period 1990–2007.

Station	Nash [–]	RMSE [m]	Bias [m]
Gien	0.99	0.09	–0.01
Orléans	0.85	0.27	–0.14
Blois	0.95	0.13	0.01
Onzain	0.90	0.26	0.23
Langeais	0.95	0.21	–0.04
Saumur	0.95	0.23	0.04

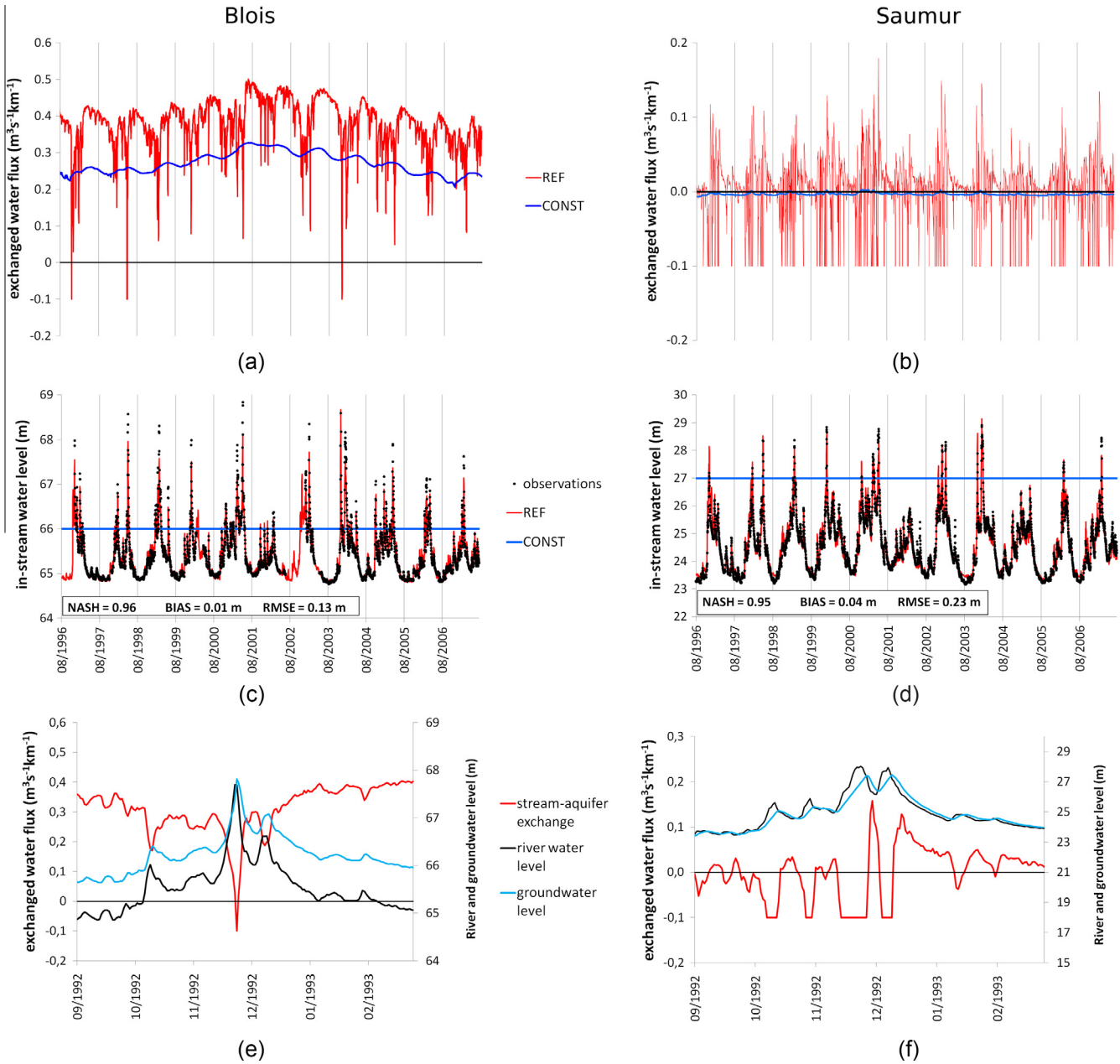


Fig. 3. Stream-aquifer exchanges (a and b) and in-stream water levels (c and d) at the stations of Blois (left panels) and Saumur (right panels), as computed by the reference (red line) and constant river stage (blue line) simulations. The observed river stages are represented by the black dots. Figures e and f compare the stream-aquifer exchanges (red line), the river water level (black line) and the piezometric head (blue line) for a 6 months period. (For interpretation of the references to color in this figure legend, the reader is referred to the web version of this article.)

Table 3

Performance of the reference simulation in terms of river discharge: statistical criteria over the period 1990–2007. Nash In denotes the Nash coefficient calculated on the natural logarithm of the discharge. Rel. Bias denotes the relative bias, i.e., the ratio between the bias and the average of the observations.

Nash [–]	Nash In [–]	Bias [$\text{m}^3 \text{s}^{-1}$]	Rel. bias [–]
Average for the 161 discharge stations			
0.65	0.53	2.09	0.10
Outlet station (Saint-Nazaire)			
0.96	0.95	36.9	0.04

peak ($0.4 \text{ m}^3 \text{s}^{-1} \text{km}^{-1}$) is simulated around the Blois station, that is, at the border between the Beauce aquifer and the outcropping of the Chalk aquifer (Fig. 6).

Globally, 72% of the network length is in gaining and 7% in losing regime, with a total net flow at the interface of $107 \text{ m}^3 \text{s}^{-1}$ (Table 6), which corresponds to a specific flow of $2 \cdot 10^{-2} \text{ m}^3 \text{s}^{-1} \text{km}^{-1}$. The total exfiltration is $125 \text{ m}^3 \text{s}^{-1}$ and the infiltration $17 \text{ m}^3 \text{s}^{-1}$. Given that the mean daily discharge at the outlet gauging station of Saint-Nazaire is $883 \text{ m}^3 \text{s}^{-1}$, the groundwater contribution to the Loire river discharge corresponds to only 12% of the Loire total discharge. As a consequence, the river network is expected to be quite sensitive to climate driven surface water changes.

4.3.2. Annual configurations

In the WY scenario, the maximum percentage of network length in gaining condition $L_{A \rightarrow S}$ is attained (76%), as a result of the decrease of both $L_{S \rightarrow A}$ and L_0 (Table 6). The total net flow increases

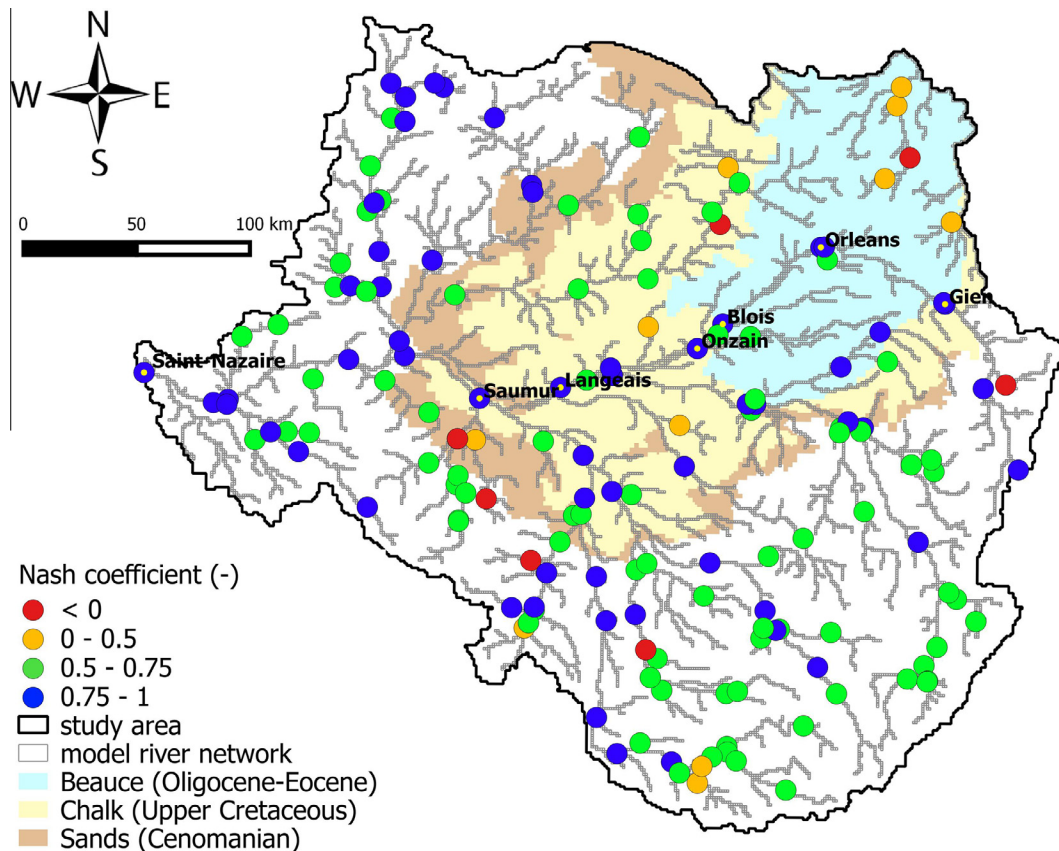


Fig. 4. Nash coefficient for river discharge in the period 1990–2007 for the reference simulation.

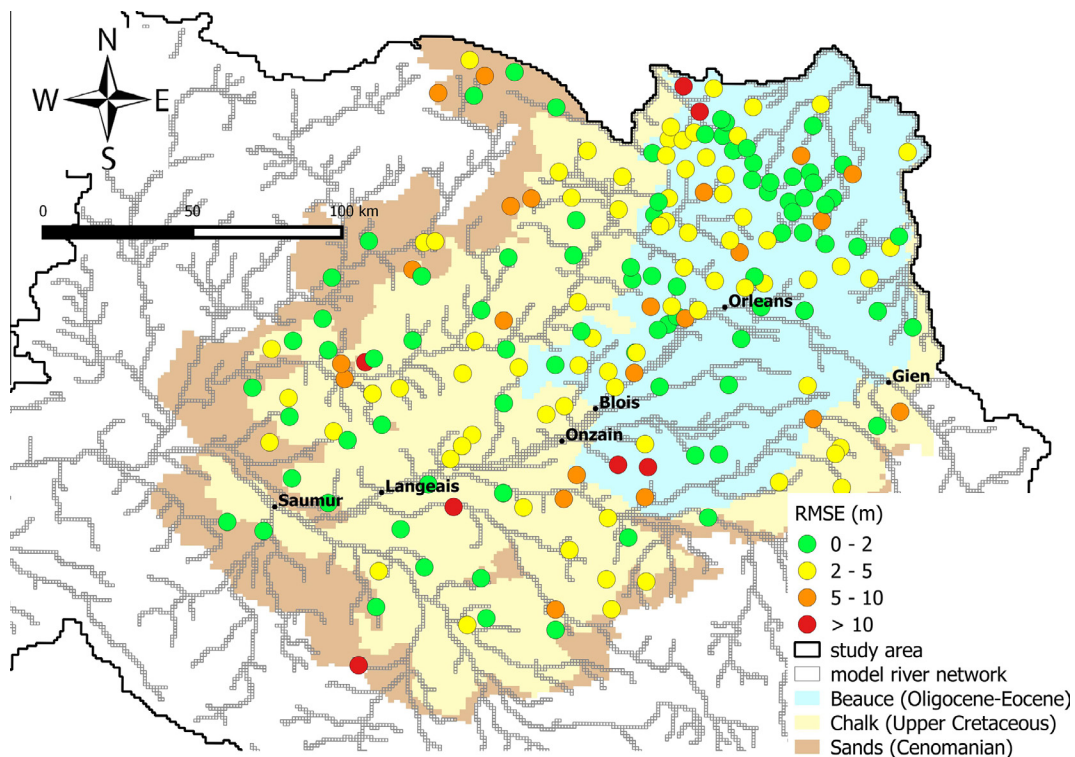


Fig. 5. RMSE for piezometric head in the period 1990–2007 for the reference simulation.

of 39% with respect to the pluri-annual value, whereas the total exfiltration increases of 40% and the total infiltration of 47% (Table 6).

In the DY scenario, 6% of the river network length switches to negligible exchange conditions, so that the percentage of network length in gaining condition decreases to 66% (Table 6). The total net

Table 4

Performance of the reference simulation in terms of piezometric head: statistical criteria over the period 1990–2007 for the three modeled aquifer units.

Aquifer	RMSE [m]	Bias [m]
Oligocene-Eocene (Beauce)	2.84	−0.86
Upper cretaceous chalk	5.22	−1.64
Cenomanian sands	5.30	0.55

flow decreases of 16% with respect to the pluri-annual value, whereas the total exfiltration decreases of 17% and the total infiltration of 18% (Table 6).

The comparison of the annual scenarios with the pluri-annual configuration shows that both the net and absolute fluxes increase during WY and decrease during DY. This is due to the higher and lower aquifer recharge occurring during the wet and dry years, respectively. The Loire basin functioning is then similar to that of the Seine river basin (Pryet et al., 2015), which is characterized by the same geological substratum and climate.

4.3.3. Short-term hydrological event configurations

A significant variation of the spatial distribution of the stream-aquifer exchanges is observed in the HF scenario, when 43% of the network length is in gaining condition and 29% is in losing condition (see Table 6 and Fig. 7). During HF, the total infiltration increases of 430% with respect to the pluri-annual value (Table 6). In fact, the stream-aquifer exchanges respond quickly to changes in surface water levels (Rosenberry et al., 2013; Diem et al., 2014). During flood periods, the river stages increase more rapidly than the groundwater levels. As a consequence, the infiltration is enhanced and flow reversals can occur in some river reaches, as discussed in Section 4.4.3.

The response of the stream-aquifer exchanges during LF is similar to that observed during DY (Table 6). Indeed, the low-flow day (11/09/1996) belongs to a rather dry hydrological year, as the mean discharge at the outlet gauging station of Saint-Nazaire is $641 \text{ m}^3 \text{ s}^{-1}$. Moreover, the low-flow day follows a period of nearly 60 days of average low-flow conditions, during which the groundwater levels decrease in response to the lower recharge. Therefore, the two extreme scenarios HF and LF represent two distinct hydrological situations. The HF scenario is characterized by an abrupt increase of river stages, during which the groundwater levels do not have time to equilibrate. The LF scenario, instead, occurs after several days of low river stages, during which the groundwater levels have enough time to react. As a consequence, the impact on the stream-aquifer exchanges is more significant during HF than during LF (Table 6).

4.4. Impact of in-stream water level fluctuations on stream-aquifer exchanges

4.4.1. Long-term impact

The assumption of constant in-stream water levels impacts the pluri-annual spatial distribution of the net stream-aquifer exchanges all along the Loire river, whereas the effect on the rest

of the network is negligible (Fig. 8a). The absolute variations of the net fluxes with respect to the reference simulation are greater than $10^{-2} \text{ m}^3 \text{ s}^{-1} \text{ km}^{-1}$, which corresponds to half the pluri-annual total net flux, for only 5% of the network length. However, the differences can locally reach values as large as $1.5 \text{ m}^3 \text{ s}^{-1} \text{ km}^{-1}$ (Fig. 8a). Moreover, the percentages of the network in average gaining and losing regime, $L_{A \rightarrow S}$ and $L_{S \rightarrow A}$, are not significantly affected by the river water dynamics (Fig. 9).

The absolute fluxes at the interface are significantly affected by river stage fluctuations (Fig. 9). Indeed, the simulation with constant river stages underestimates the pluri-annual exfiltration and infiltration of 10% and 70%, respectively (Table 7). This result is explained by the fact that the constant river stages cannot represent the high-flow periods properly, which favor infiltration, and the low-flow periods, which favor the exfiltration. On the other hand, the impact on the average net flux Q_{net} is negligible (Fig. 9 and Table 7).

A similar pattern is simulated in the annual scenarios (WY and DY, Fig. 9): $L_{A \rightarrow S}$, $L_{S \rightarrow A}$ and L_0 are minimally impacted and the absolute fluxes are significantly underestimated. Moreover, differently from the pluri-annual scenario, the impact on the net flux is not negligible.

In particular, during WY, the infiltration decreases more than the exfiltration. In fact, the constant river stages underestimate the high-flow river stages even more significantly during a wet year than in pluri-annual average conditions. As a consequence, the net flux is overestimated of 3.4% with respect to the reference simulation (Table 7).

Conversely, during DY, the exfiltration decreases more than the infiltration. In fact, the constant river stages overestimate the low-flow river stages even more significantly during a dry year than in pluri-annual average conditions. As a consequence, the net flux is underestimated of 2% with respect to the reference simulation (Table 7).

4.4.2. Short-term impact

The impact of river stage fluctuations during a single hydrological event is even more important than for the pluri-annual or annual configurations. Indeed, not only the absolute fluxes, but also the net flux and the spatial distribution of the exchanges are significantly affected.

During HF, the simulation with constant river stages overestimates of 28% the length of the river network in gaining condition, $L_{A \rightarrow S}$, and underestimates of 23% the length of the river network in losing condition, $L_{S \rightarrow A}$ (Table 7). In fact, during high-flow the constant river stages are generally lower than the real values (Fig. 3c and d) so that exfiltration is favored against infiltration. The total exfiltration is then overestimated of 54% and the total infiltration is underestimated of 84%. The net flow is overestimated of $130 \text{ m}^3 \text{ s}^{-1}$ (Fig. 9), i.e., it is almost twenty times the reference value (Table 7).

During LF, the total exfiltration is underestimated of 8%, the total infiltration is underestimated of 60% and the net flow is underestimated of 1.6% (Table 7). During low-flow, the constant

Table 5

Calibration of the Manning coefficient along the Loire river. \bar{n} is defined by Eq. (8) as described in the text. n_0 denotes the parameter of the reference simulation.

Station	$\bar{n} [\text{s m}^{-1/3}]$	RMSE(\bar{n}) [m]	RMSE($n = 0.025 \text{ s m}^{-1/3}$) [m]	$n_0 [\text{s m}^{-1/3}]$
Saumur	0.026	0.09	0.12	0.026
Langeais	0.032	0.24	0.51	0.032
Onzain	0.016	0.29	0.18	0.025
Blois	0.016	0.11	0.31	0.016
Orléans	0.033	0.32	0.29	0.025
Gien	0.015	0.04	0.61	0.015

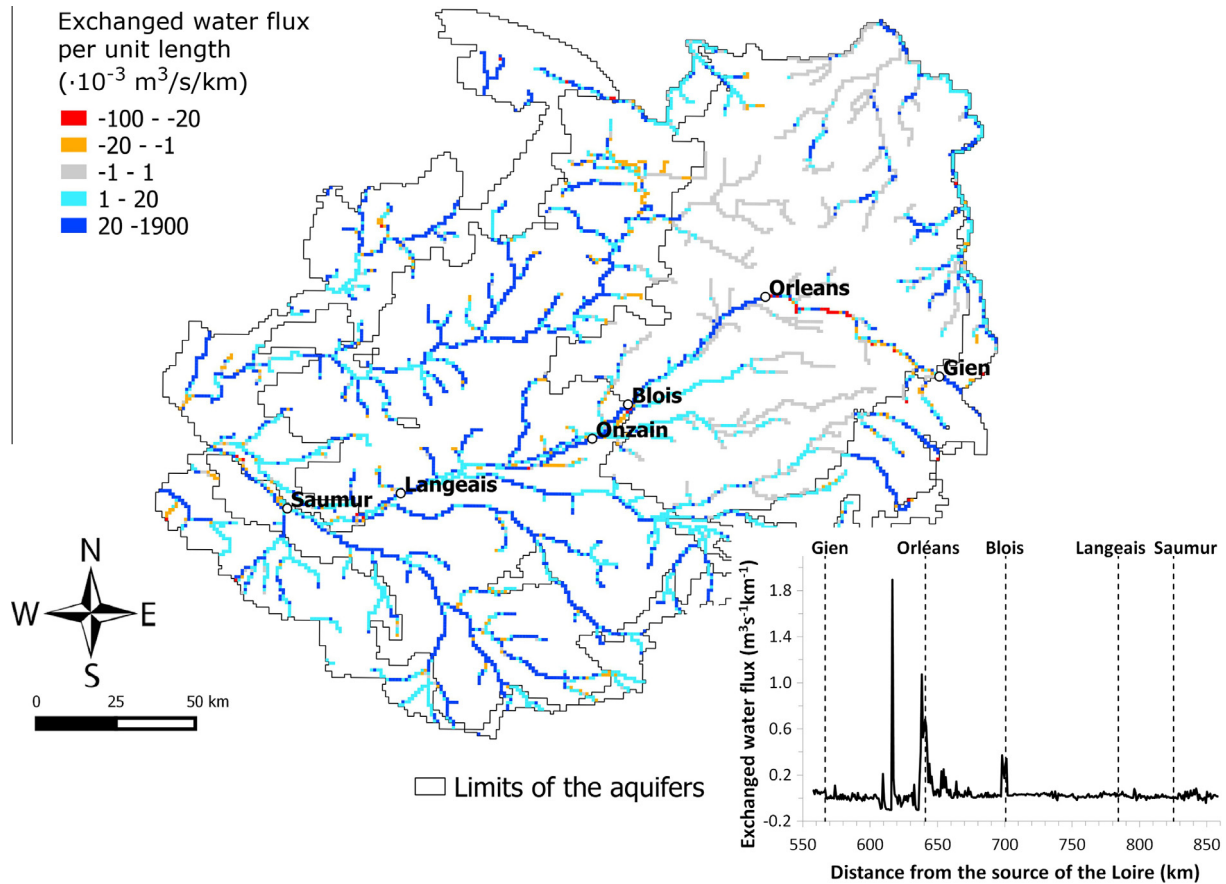


Fig. 6. Average stream-aquifer exchanges (reference simulation, 1990–2007). The inset focuses on the Loire river.

Table 6

Total stream-aquifer exchanges for the whole simulated river network and the different scenarios of the reference simulation (PA: pluri-annual, WY: wet year, DY: dry year, HF: high-flow, LF: low-flow). Q_{net} is the net flux, $Q_{A \rightarrow S}$ is the exfiltrating flux (aquifer to river) and $Q_{S \rightarrow A}$ is the infiltrating flux (river to aquifer). L_0 denotes the percentage of the network length with negligible exchanges, while $L_{A \rightarrow S}$ and $L_{S \rightarrow A}$ are the percentages of the network length in average gaining or losing conditions, respectively.

	Q_{net} [$m^3 s^{-1}$]	$Q_{A \rightarrow S}$ [$m^3 s^{-1}$]	$Q_{S \rightarrow A}$ [$m^3 s^{-1}$]	L_0 [%]	$L_{A \rightarrow S}$ [%]	$L_{S \rightarrow A}$ [%]
PA	107.1	124.5	17.4	21.7	71.8	6.5
WY	148.4	173.9	25.5	19.3	76.1	4.6
DY	89.8	103.9	14.2	27.9	66.0	6.2
HF	7.0	98.9	91.9	27.5	43.3	29.2
LF	85.4	96.2	10.8	36.8	58.7	4.5

river stages are generally higher than the real values (Fig. 3c and d), which explains the underestimation of the exfiltration.

In-stream water level fluctuations impact the stream-aquifer exchanges more significantly in the HF scenario than in the LF scenario. In fact, the river network is globally in gaining regime, so that flow reversals can occur during high-flow periods. Moreover, the difference between constant river stages and real river stages is generally more important during high-flow than low-flow (Fig. 3c and d).

4.4.3. Time variability of the exchanged fluxes

The high-frequency river stage variations give rise to an increased variability of the stream-aquifer exchanges with respect to the simulation performed with constant river stages and to possible flow reversals during hydrological events (Fig. 3a and b).

Different responses of the stream-aquifer exchanges are observed according to the average difference between piezometric head and river stage. For example, the Blois station (Fig. 2) is characterized by an average exfiltrating regime, with an average net flux of $3.7 \cdot 10^{-1} m^3 s^{-1} km^{-1}$. The time series of the river stages

and of the stream-aquifer exchanges (Fig. 3a and b) are inversely correlated ($r = -0.8$). On the other hand, the Saumur station (Fig. 2) is also in average exfiltrating regime, but with an average net flux of $3.7 \cdot 10^{-3} m^3 s^{-1} km^{-1}$, that is, two orders of magnitudes lower than the Blois station. This station is characterized by a situation of quasi-equilibrium between the river stage and the piezometric head (Fig. 3f). This configuration implies that the stream-aquifer exchanges are highly sensitive to the river stage variations. Differently from a clear gaining river stretch, for which the flow reversals occur during flood events only, the river stage fluctuations for river stretches at equilibrium with the nearby aquifer induce more frequent flow reversals, as displayed at the Saumur station (3b). At this gauging station, the river stages and the stream-aquifer exchanges have a much lower correlation coefficient ($r = -0.2$). In this case, a hydrological event induces first the rise of in-stream water level favoring river infiltration. In a second time, when the in-stream water level decreases, the piezometric head is still increasing due to the inertia of the groundwater system, which systematically generates a higher exfiltration rate a few days after the higher infiltration rate (3f).

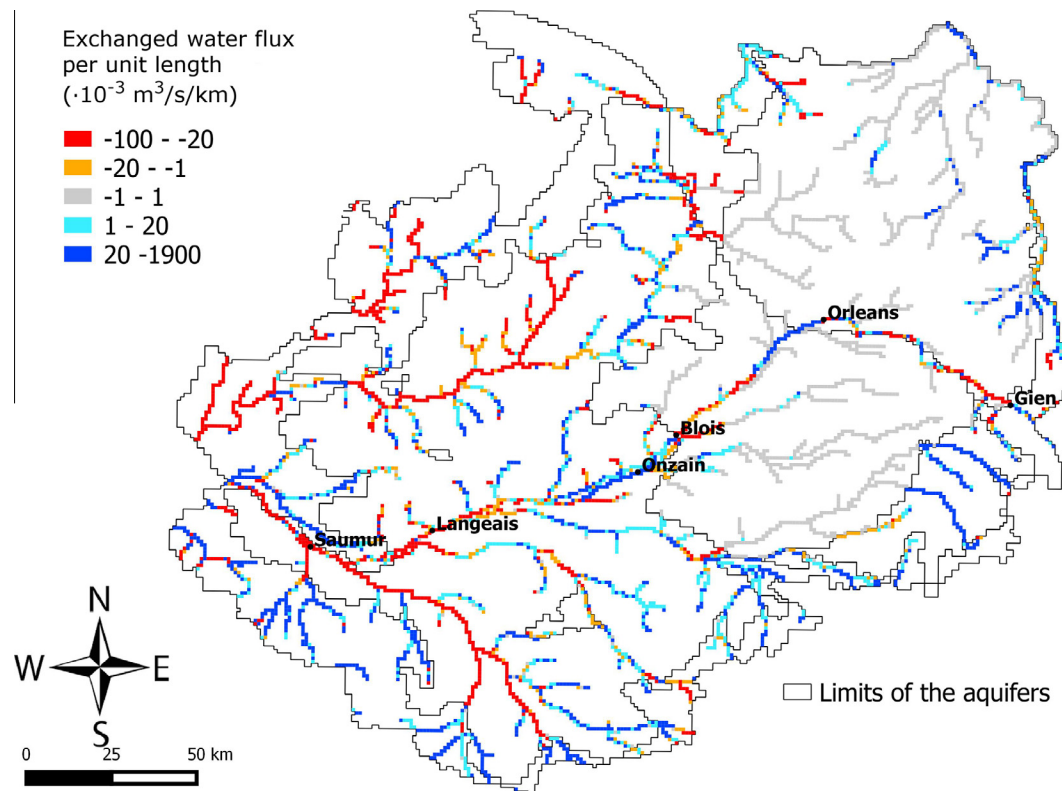


Fig. 7. Stream-aquifer exchanges estimated by the reference simulation in the high-flow condition (28/01/1995).

4.5. Sensitivity of the stream-aquifer exchanges

4.5.1. The riverbed elevation: effect of the DEM

4.5.1.1. Long-term impact. The usage of the SRTM3 DEM to estimate the riverbed elevation significantly impacts the spatial distribution of the pluri-annual net fluxes (Fig. 8b). The absolute variations of the net fluxes with respect to the reference simulation are greater than $10^{-2} \text{ m}^3 \text{ s}^{-1} \text{ km}^{-1}$ for 24% of the network length. These variations show a rather random pattern, and no zones of systematic underestimation or overestimation can be identified. This pattern is moderately anti-correlated ($r = -0.3$) to the distribution of the differences between the riverbed elevations computed with the SRTM3 DEM and the reference values. The negative correlation coefficient is coherent with the observation that an underestimation of the riverbed elevation implies an underestimation of the river stage, and, therefore, an overestimation of the net fluxes. The local variations tend to balance out, so that the total net flux is overestimated of 3% only for both the pluri-annual and annual configuration. The absolute fluxes are overestimated by approximately the same percentage (Table 7). As the fractions of the stream network in gaining and losing regime do not change significantly (Fig. 9), the increase of the total net and absolute fluxes is due to the increase of the local fluxes at the river cell scale. The increase of the total net flow of the system is in agreement with the fact that, on average, the riverbed elevations estimated with the SRTM3 DEM are lower than the reference values (Section 3.4.3).

4.5.1.2. Short-term impact. Contrary to the annual and pluri-annual results, the usage of the SRTM3 derived DEM in the HF scenario leads to an underestimation of the total exfiltration (-7.8%), while the total infiltration is overestimated of the same percentage (Table 7 and Fig. 9). As a consequence, the net flux is underestimated (-200%) and becomes negative, that is, the river network is globally in losing regime. The impact of the riverbed elevation is less significant in the LF scenario (Fig. 9).

4.5.2. The riverbed roughness: effect of the Manning coefficient

4.5.2.1. Long-term impact. The perturbation of the Manning coefficient values does not affect the spatial distribution of the pluri-annual exchanges significantly, except for the reaches of the Loire river around Orléans and between Blois and Onzain (Fig. 8c). Those are also the reaches characterized by the most intense exchanges according to the reference simulation (Fig. 6). The pluri-annual total net fluxes differ of more than $10^{-2} \text{ m}^3 \text{ s}^{-1} \text{ km}^{-1}$ from the reference values for 1.4% of the network length only.

Decreasing the Manning coefficient of 20% of its reference value leads to an underestimation of the pluri-annual total absolute fluxes up to 7.5%. Conversely, the increase of the Manning coefficient of 20% determines the overestimation of the total absolute fluxes up to 18% (Table 7).

The increase of the riverbed roughness implies an increase of the river stages and, therefore, a more intense infiltration. This is in agreement with the fact that the infiltration simulated increases with the value of n . The infiltrated water recharges the aquifer during high-flow periods and determines a rise of the piezometric head leading to a more intense exfiltration in low-flow periods (Flipo et al., 2014; Bendjoudi et al., 2002). This is the reason why the exfiltration simulated also increases with n (Fig. 9).

For both negative and positive perturbations of n , the variation of the absolute fluxes compensates each other, so that the impact of n on the pluri-annual total net flow is negligible (Fig. 9) and does not exceed 0.5% of the reference value (Table 7).

The effect of the riverbed roughness in the WY and DY scenarios is similar to that observed in the pluri-annual configuration (Fig. 9 and Table 7).

The stream-aquifer exchanges are generally more sensitive to positive than to negative perturbations of n . This result was unexpected, as Eq. (4) shows that the river depth is a function of $n^{3/5}$, so that the river stages variations are more important when n is decreased by 20% than when it is increased by 20%. However, the hydrosystem is globally in gaining regime, so that the increase of

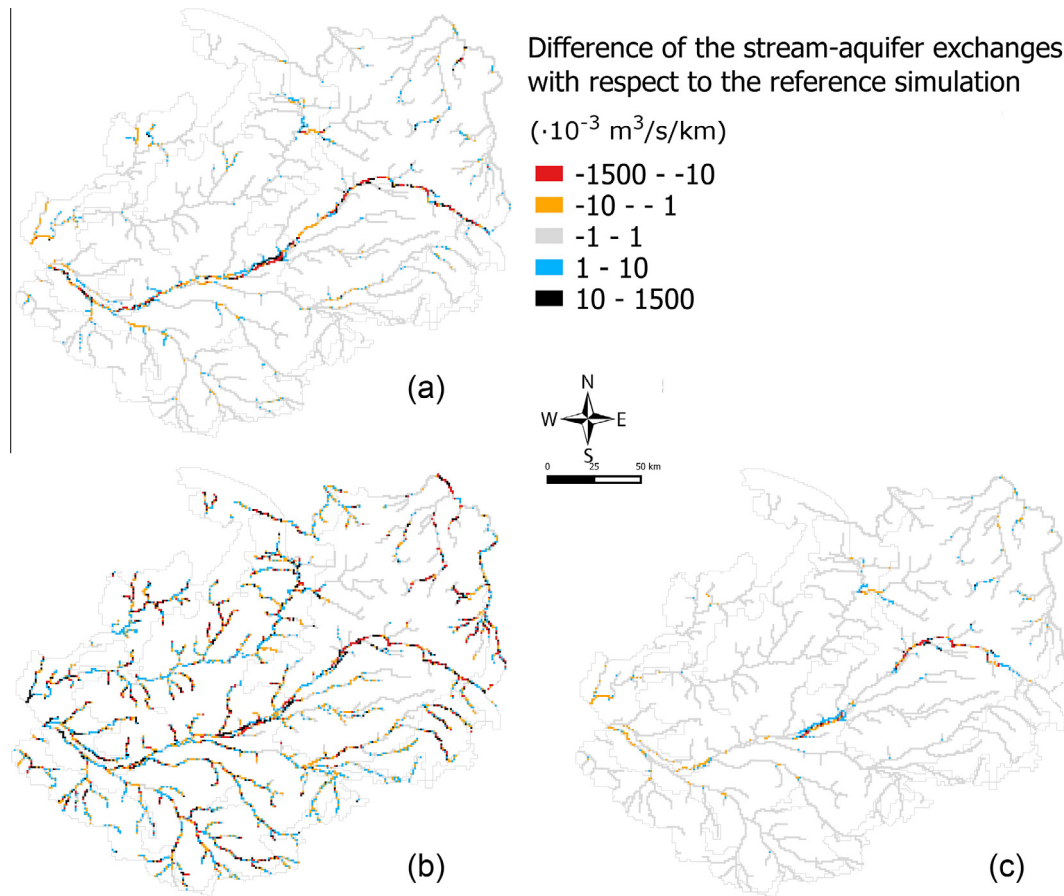


Fig. 8. Variation of the pluri-annual stream-aquifer exchanges with respect to the reference simulation for the simulation with constant river stages (a), SRTM3 digital elevation model (b) and Manning coefficient modified by +20% (c).

the river stages, determined by the increase of the Manning coefficient, can lead to flow reversals.

4.5.2.2. Short-term impact. In the HF scenario, the modification of the riverbed roughness leads to an underestimation of the net flow for both negative and positive variations of n (Fig. 9). The direction of the total net flux is reversed in both cases, so that the river system switches to average losing conditions.

The impact of the perturbation of the Manning coefficient on the stream-aquifer exchanges is less important in the LF scenario than in the HF scenario (Fig. 9). The only exception is represented by the quantities characterizing the network configuration ($L_{A \rightarrow S}$, $L_{S \rightarrow A}$, L_0) when n is decreased by 20%. In fact, 1.6% of the network length switches from losing or negligible exchange condition to gaining condition (Fig. 9). The exfiltration is overestimated for both positive and negative perturbations of n (Fig. 9 and Table 7). As previously observed, this is due to the increased aquifer recharge during high-flow periods.

5. Discussion

5.1. Relative sensitivity of the stream-aquifer exchanges

The results of the sensitivity analysis highlight that in-stream water level fluctuations, the DEM and the Manning coefficient have different effects on the estimation of stream-aquifer exchanges.

In-stream water level fluctuations have the most significant effect on the estimation of the total absolute fluxes at regional scale. The assumption of constant river stages leads to an underes-

timization by 10% of the pluri-annual exfiltration and by 70% of the pluri-annual infiltration. The underestimation is even more important during wet years (WY scenario) and short-term high-flow periods (HF scenario). The impact on the net flux is less important, and is observed only at annual (or shorter) time scales. The same pattern was simulated for a 17,000 km² sub-basin of the Seine river basin (Saleh et al., 2011) coupling Eau-Dyssée with a 1D Saint Venant hydrological model. Moreover, the river stage fluctuations enhance the time variability of the stream-aquifer exchanges and can trigger flow reversals during flood events and also more frequently for river stretches at equilibrium with its nearby aquifer.

The usage of the coarser resolution SRTM3 DEM to estimate the riverbed elevation has the most significant impact on the estimation of stream-aquifer exchanges at local scale: for 24% of the river network, the net flux differs from the reference value for more than $10^{-2} \text{ m}^3 \text{ s}^{-1} \text{ km}^{-1}$, which corresponds to half the averaged total net exchange rate of the basin. Such local variations tend to compensate at regional scale, as the riverbed elevations derived from the SRTM3 DEM differ from the reference values with a rather random spatial pattern. Despite the compensation of the local variations, the impact on the pluri-annual net flux at regional scale is the most significant among the simulation analyzed. In fact, Q_{net} is overestimated by 2.5%.

Even if the riverbed roughness affects the timing of infiltration and exfiltration, it has a minor impact on the stream-aquifer exchanges with respect to the other parameters (river stage fluctuations and riverbed elevation). A perturbation of the Manning coefficient by 20% of the reference values leads to an overestimation of the pluri-annual and annual total absolute fluxes up to 18%. On the contrary, the impact on the total net flux is less significant and

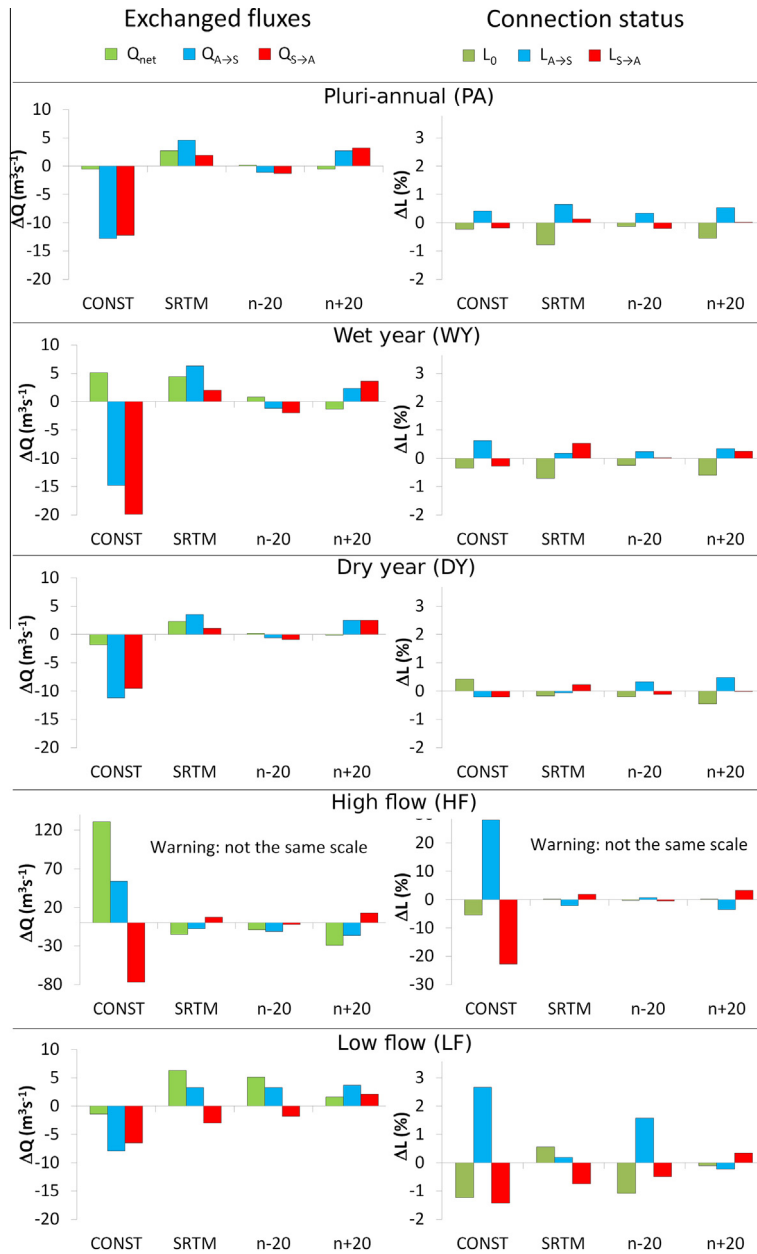


Fig. 9. Graphs on the left: absolute difference of water fluxes ΔQ , for net flux (Q_{net}), exfiltration ($Q_{A \rightarrow S}$), infiltration ($Q_{S \rightarrow A}$). Graphs on the right: absolute difference of the percentage of the network length ΔL in infiltrating ($L_{A \rightarrow S}$), infiltrating ($L_{S \rightarrow A}$) and negligible exchange (L_0) condition. The differences are with respect to the reference simulation. The scales are different for the graphs in the high-flow scenario. CONST: simulation with constant river stages, SRTM: simulation with the riverbed elevation derived from the SRTM3 DEM, n - 20 (n + 20): simulation with the Manning coefficient decreased (increased) of 20%.

does not exceed 0.9% of the reference values. The minor impact of the riverbed roughness is probably due to the fact that the river stages change less with respect to the reference values when the Manning coefficient is perturbed by 20% than in case of constant river stages or perturbed riverbed elevation. Considering the 6 gauging stations along the Loire river, the bias with respect to the reference river stages is 1.6 m for the simulation with constant river stages, -3.5 m for the simulation with the riverbed elevation derived from the SRTM3 DEM, -0.19 m for the simulation with the Manning coefficient decreased by 20% and 0.17 m for the simulation with the Manning coefficient increased by 20%.

The average distribution of infiltrating and exfiltrating cells, that is the values of $L_{A \rightarrow S}$, $L_{S \rightarrow A}$ and L_0 , is not significantly sensitive to the processes analyzed, except during short-term hydrological events. This result is consistent with the fact that at regional scale the stream-aquifer exchanges are primarily controlled by the

regional groundwater flow paths and by the large scale structural heterogeneities (Flipo et al., 2014).

The high-flow and the wet year resulted to be the most sensitive scenarios among those analyzed for all the simulations considered. This is due to the fact that the hydrosystem is, in average, in gaining condition. Therefore, during high-flow and wet years the probability of flow reversals at the stream-aquifer interface increases with respect to average, low-flow and dry year conditions.

5.2. Establishing a hierarchy of the processes governing the estimation of distributed stream-aquifer exchanges at regional scale

The results of this study highlight a hierarchy between the processes and parameters which govern the estimation of stream-aquifer exchanges at regional scale with a distributed

Table 7

Relative differences (in %) with respect to the reference simulation. This table complements Fig. 9.

	Q_{net}	$Q_{A \rightarrow S}$	$Q_{S \rightarrow A}$	L_0	$L_{A \rightarrow S}$	$L_{S \rightarrow A}$
<i>Constant in-stream water levels</i>						
PA	−0.5	−10	−70	−1	0	−3.8
WY	3.4	−8.5	−78	−3.7	0.7	−11
DY	−2	−11	−67	−0.6	−0.2	−2.2
HF	$2 \cdot 10^3$	54	−84	−20	63	−77
LF	−1.6	−8.2	−60	−3.4	5.8	−30
<i>Coarser DEM (SRTM3)</i>						
PA	2.5	3.7	11	−3.6	0.8	2.5
WY	3.0	3.6	7.8	−3.7	0.4	7.5
DY	2.6	3.4	7.7	−0.6	−0.2	2.2
HF	$-2 \cdot 10^2$	−7.8	7.9	0.8	−4.7	6
LF	7.4	3.4	−28	1.5	−0.2	−17
<i>Manning coefficient decreased of 20%</i>						
PA	0.2	−0.9	−7.5	−0.6	0.5	−1.3
WY	0.5	−0.7	−7.8	−1.3	0.4	−1.9
DY	0.2	−0.6	−6.3	−0.7	0.2	−1.1
HF	$-1 \cdot 10^2$	−11	−2.3	−1	1.8	−0.3
LF	6	3.4	−17	−2.9	2.8	−13
<i>Manning coefficient increased of 20%</i>						
PA	−0.5	2.2	18	−2.5	0.8	0
WY	−0.9	1.3	14	−3.1	0.7	0
DY	−0.1	2.4	18	−1.6	0.4	1.1
HF	$-4 \cdot 10^2$	−16	14	0.8	−8.4	11
LF	1.9	3.8	19	−0.3	−0.2	8.5

surface–subsurface model. The hierarchy arises from the analysis of the spatial distribution of the pluri-annual total net fluxes as well as from the analysis of quantities characterizing the fluxes in the entire hydrosystem ($Q_{A \rightarrow S}$, $Q_{S \rightarrow A}$, Q_{net} , $L_{A \rightarrow S}$, $L_{S \rightarrow A}$ and L_0) at different time scales (pluri-annual, annual, daily).

First of all, distributed hydrological–hydrogeological models need to take into account the river stage fluctuations for two main reasons. The first is to evaluate the absolute fluxes (exfiltration and infiltration) at the stream–aquifer interface correctly. The second is to reproduce the dynamics of the stream–aquifer exchanges at different time scales and, specifically, the situations of flow reversal.

This is of primary importance for transport problems at the stream–aquifer interface. Indeed, the regional net and absolute fluxes affect the hyporheic exchange, the solute fluxes and the biogeochemical reactions (Trauth et al., 2015). The hyporheic exchanges and the denitrification during bank storage are more efficient under equilibrium condition than under gaining or losing conditions (Trauth et al., 2015). The importance of river stage fluctuations for riparian denitrification during bank storage between flood events has also been highlighted by Knight and Rassam (2007).

Secondly, an accurate estimation of the riverbed elevation is important in order to correctly evaluate the pluri-annual total net flux and the spatial variability of the stream–aquifer exchanges. It is therefore crucial to develop accurate high resolution DEM at regional scale, or to develop alternative methods to estimate the riverbed elevation (see Section 5.3.1).

Topography and hydrogeomorphology have shown to be important for the hydrologic response of a basin (Mejia and Reed, 2011), for the estimation of residence times and surface–subsurface interactions at different scales (McGuire et al., 2005; Wörman et al., 2007), for water quality, biodiversity and river ecosystem functioning (Elosegi and Sabater, 2013), as well as for the estimation of the hyporheic exchange flow (Shope et al., 2012; Käser et al., 2014). Hyporheic exchange flow affects biogeochemical reactions at the stream–aquifer interface (Trauth et al., 2015) and stream temperature (Arrigoni et al., 2008).

The estimation of the riverbed roughness has minor priority with respect to the other factors analyzed in this work. A calibration of this parameter should then be done only after having

realized the two previous steps or in case a precise local estimation of the stream–aquifer exchanges is needed in a specific site.

5.3. Further research

5.3.1. Riverbed elevation

The results of this paper emphasise the importance of accounting for in-stream water level fluctuations in regional scale hydrosystem models. The modeling approach, which is based on the Manning equation, requires the knowledge of the distribution of river width, riverbed elevation and slope as well as of the Manning roughness coefficient. The sensitivity analysis has highlighted the significant impact of the riverbed elevation on the quantification of the stream–aquifer exchanges. It is then mandatory to develop new methodologies to better estimate the riverbed elevation at high resolution for a stream network at regional scale. In this sense, remote sensed images represent a promising tool. New space borne products such as Surface Water and Ocean Topography (SWOT) satellite mission will provide alternative tools to DEM usage for the simulation of stream–aquifer exchanges at the regional scale. Indeed, SWOT will provide measurements of water surface elevation, width and slope for rivers wider than 50 m (Biancamaria et al., 2016). These data can be used as input to inverse models to retrieve the riverbed elevation, roughness coefficient and then river discharge. Algorithms of this kind have already been developed and applied using synthetic SWOT data (Garambois and Monnier, 2015; Durand et al., 2014, 2010). The usage of such algorithms coupled with our approach should lead to significant improvements of the simulation of stream–aquifer interactions at the regional scale.

Further work is also needed to evaluate the sensitivity of the stream–aquifer exchanges to the river width and riverbed slope. The distribution of river widths at regional or larger scale can be obtained through semi-automated and automated techniques using remotely sensed images (Pavelsky and Smith, 2008; Yamazaki et al., 2014). Moreover, the SWOT satellite mission will improve such estimates by providing time dependent distributions of river width and slope. Such technological breakthrough will also contribute to the improvement of the quantification of stream–aquifer exchanges at the regional scale.

5.3.2. Maximum infiltration rate

According to the modeling approach used in this study, the infiltration rate is limited by a maximum value, Q_{lim} , which is considered uniform along the whole river network. The role of this coefficient depends on the climatic conditions. In arid climates, Q_{lim} represents the infiltration occurring by gravity in a disconnected hydrosystem (Brunner et al., 2009; Rivi re et al., 2014; Xie et al., 2014).

In temperate climates, Q_{lim} also represents a limit to the infiltration rate during floods. In fact, during flood events, the river stages modeled with the Manning-Strickler approach overestimate the real river stages for two reasons. First, the inundation of the floodplain is not taken into account. Secondly, the roughness coefficient is assumed to be constant, although flood events tend to remove the sediments at the riverbed and then to decrease its roughness. As a consequence, the infiltration rate calculated with Eq. (1) would overestimate the real infiltration rate. Such overestimation is prevented by imposing the maximum infiltration rate Q_{lim} . In other words, this coefficient compensates for the approximation errors of the rating curve. The limitations of the conductance model in describing the infiltration during flood events was also highlighted by Engeler et al. (2011).

The parameter Q_{lim} could bias the sensitivity analysis of the infiltrating flux. In fact, once the infiltration rate has reached Q_{lim} , it becomes independent on further increases of river stages during hydrological events. Further research is then needed to evaluate the impact of this parameter on the quantification of the distributed stream-aquifer exchanges for long and short periods of time. Saleh et al. (2011) showed that Q_{lim} has a negligible impact on the average net stream-aquifer exchange over a 5 years period. This is due to their upscaling methodology based on a 1D Saint-Venant hydraulic model, which takes into account the floodplain. Such methodology is therefore less sensitive to Q_{lim} than a pure Manning-Strickler approach for which in-stream water levels continue to rise at the same speed even when overflowing. For short periods of time, such as flood events, the role of Q_{lim} needs to be assessed.

Moreover, it is necessary to develop methods to estimate the spatial distribution of Q_{lim} at regional scale, for example by defining this parameter as a function of the properties of the stream bed and of the regional aquifer, as suggested by Flipo et al. (2014). This is a task of primary importance for the quantification of stream-aquifer exchanges both for arid climates, where disconnection is more frequent, and for temperate climates during flood events.

6. Conclusions

An estimation of the stream-aquifer exchanges has been achieved at a 1 km resolution over a 5000 km river network in the Loire basin. Water fluxes have been computed with a conductance model, in which river stage fluctuations were taken into account with a simplified Manning-Strickler approach. The effects of river stage fluctuations on the estimations of stream-aquifer exchanges have been assessed by analyzing the results of a simulation with constant in-stream water levels, which is the common approach used in regional scale hydrosystem modeling. A sensitivity analysis was performed to evaluate the effects of the uncertainties related to the DEM, which in turn affects the estimation of the riverbed elevation, and to the Manning roughness coefficient.

The regional model reproduced in-stream water level fluctuations of the main river with excellent accuracy at the scale of the single gauging stations.

The sensitivity analysis showed the importance of accounting for river stage fluctuations in the modeling of regional hydrosys-

tems. In fact, the assumption of constant river stages leads to a significant underestimation of the total infiltration and exfiltration in the basin, whereas it has a negligible influence on the pluri-annual net flux. Moreover, the river fluctuations increase the time variability of the stream-aquifer exchanges and may determine flow reversals in high-flow periods. Accounting for in-stream water level fluctuations is therefore crucial for transport issues, as the exchanges of matter between the surface and subsurface depend on the flow dynamics at the stream-aquifer interface.

The DEM, which is used to estimate the riverbed elevation, significantly impacts the local estimation of the stream-aquifer exchanges all along the river network. Therefore, it is of major importance to develop new methodologies to improve the high-resolution estimation of the riverbed elevation at regional scale.

The Manning roughness coefficient is the least sensitive parameter. Errors on Manning coefficient affect the timing of infiltration and exfiltration leading to temporally localized discrepancies, which do not affect the global net estimates significantly.

The sensitivity analysis indicates that the uncertainties affecting the riverbed elevation and the Manning coefficient do not weaken the importance of accounting for in-stream water level fluctuations in regional scale hydrosystem modeling. Further work is needed to evaluate the sensitivity of the stream-aquifer exchanges to the river width, riverbed slope and to the maximum infiltration rate.

Acknowledgements

This work was part of the scientific program 'Control factors of river temperature at regional scale in the Loire catchment' funded by European funds (FEDER, Fonds Europ ens de D veloppement R gional), Etablissement Public Loire and the Loire River Basin Authority (Agence de l'Eau Loire Bretagne). The first author is now funded by the CNES TOSCA SWOT research project. The authors warmly thank Florence Curie, Aur lien Beaufort and Eric Lalot (University of Tours) and Michel Poulin (MINES ParisTech) for the useful discussions on the Loire system functioning. Baptiste Labarthe (MINES ParisTech) and C line Monteil (EDF R&D) are also thanked for their help in the usage of the EauDyss e model.

References

- Arrigoni, A., Poole, G., Mertes, L., O'Daniel, S., Woessner, W., Thomas, S., 2008. Buffered, lagged, or cooled? Disentangling hyporheic influences on temperature cycles in stream channels. *Water Resour. Res.* 44, W09418.
- Battle-Aguilar, J.B., Morasch, B., Hunkeler, D., Brouy re, S., 2014. Benzene dynamics and biodegradation in alluvial aquifers affected by river fluctuations. *Ground Water* 52, 388–398.
- Bendjoudi, H., Weng, P., Gu rin, R., Pastre, J., 2002. Riparian wetlands of the middle reach of the Seine river (France): historical development, investigation and present hydrologic functioning. A case study. *J. Hydrol.* 263, 131–155.
- Biancamaria, S., Lettenmaier, D.P., Pavelsky, T.M., 2016. The SWOT mission and its capabilities for land hydrology. *Surv. Geophys.* 37, 307. <http://dx.doi.org/10.1007/s10712-015-9346-y>.
- Brunner, P., Simmons, C., Cook, P., 2009. Spatial and temporal aspects of the transition from connection to disconnection between rivers, lakes and groundwater. *J. Hydrol.* 376, 159–169.
- Chery, J.L., 1983.  tude hydrochimique d'un aquif re karstique aliment  par perte de cours d'eau (la Loire): le syst me des Calcaires de Beauce sous le Val d'Orl ans Ph.D. thesis. Universit  d'Orl ans.
- Chow, V.T., 1959. *Open Channel Hydraulics*. McGraw Hill Company Inc., New York.
- Cloutier, C.A., Buffin-B langer, T., Larocque, M., 2014. Controls of groundwater floodwave propagation in a gravelly floodplain. *J. Hydrol.* 511, 423–431.
- David, C., Habets, F., Maidment, D., Yang, Z.-L., 2011a. RAPID applied to the SIM-France model. *Hydrol. Process.* 25 (22), 3412–3425.
- David, C.H., Maidment, D.R., Niu, G.-Y., Yang, Z.-L., Habets, F., Eijkhout, V., 2011b. River network routing on the NHDPlus Dataset. *J. Hydrometeorol.* 12, 913–934.
- David, C.H., Yang, Z.-L., Famiglietti, J.S., 2013. Quantification of the upstream-to-downstream influence in the Muskingum method and implications for speedup in parallel computations of river flow. *Water Resour. Res.* 49, 2783–2800.
- de Marsily, G., 1986. *Quantitative Hydrogeology - Groundwater Hydrology for Engineers*. Academic Press, London.

- de Marsily, G., Ledoux, E., Levassor, A., Poitral, D., Salem, A., 1978. Modelling of large multilayered aquifer systems: theory and applications. *J. Hydrol.* 36, 1–34.
- Deschênes, J., Villeneuve, J.-P., Ledoux, E., Girard, G., 1985. Modeling the hydrologic cycle: the MC model. Part I - Principles and description. *Nordic Hydrol.* 16, 257–272.
- Diem, S., Renard, P., Schirmer, M., 2014. Assessing the effect of different river water level interpolation schemes on modeled groundwater residence times. *J. Hydrol.* 510, 393–402.
- Dooze, J., 1968. The hydrologic cycle as a closed system. *Int. Assoc. Sci. Hydrol. Bull.* 13 (1), 58–68.
- Dunne, T., Leopold, L., 1978. *Water in Environmental Planning*. W.H Freeman and Co., San Francisco, CA.
- Durand, M., Neal, J., Rodríguez, E., Andreadis, K.M., Smith, L.C., Yoon, Y., 2014. Estimating reach-averaged discharge for the River Severn from measurements of river water surface elevation and slope. *J. Hydrol.* 511, 92–104.
- Durand, M., Rodríguez, E., Alsdorf, D.E., Trigg, M., 2010. Estimating river depth from remote sensing swath interferometry measurements of river height, slope, and width. *IEEE J. Sel. Top. Appl.* 3 (1), 20–31.
- Elosegi, A., Sabater, S., 2013. Effects of hydromorphological impacts on river ecosystem functioning: a review and suggestions for assessing ecological impacts. *Hydrobiologia* 712, 129–143.
- Engeler, I., Hendricks Franssen, H., Müller, R., Stauffer, F., 2011. The importance of coupled modelling of variably saturated groundwater flow-heat transport for assessing river-aquifer interactions. *J. Hydrol.* 397 (3–4), 295–305.
- EU Parliament, 2008. Directive 2008/105/EC of the European Parliament and of the Council of 16 December 2008 on environmental quality standards in the field of water policy, amending and subsequently repealing. *Off. J. Eur. Union* L348, 84–97.
- Farr, T.G., Rosen, P.A., Caro, E., Crippen, R., Duren, R., Hensley, S., Kobrick, M., Paller, M., Rodriguez, E., Roth, L., Seal, D., Shaffer, S., Shimada, J., Umland, J., Werner, M., Oskin, M., Burbank, D., Alsdorf, D., 2007. The shuttle radar topography mission. *Rev. Geophys.* 45, RG2004. <http://dx.doi.org/10.1029/2005RG000183>.
- Fleckenstein, J., Krause, S., Hannah, D., Boano, F., 2010. Groundwater-surface water interactions: new methods and models to improve understanding of processes and dynamics. *Adv. Water Resour.* 33 (11), 1291–1295.
- Flipo, N., June 2013. Modélisation des hydrosystèmes continentaux pour une gestion durable de la ressource en eau. Ph.D. thesis, Université Pierre et Marie Curie, Paris VI, Habilitation thesis. http://tel.archives-ouvertes.fr/docs/00/87/94/49/PDF/flipo2013_hdr.pdf.
- Flipo, N., Monteil, C., Poulin, M., de Fouquet, C., Krimissa, M., 2012. Hybrid fitting of a hydrosystem model: long term insight into the Beauce aquifer functioning (France). *Water Resour. Res.* 48, W05509.
- Flipo, N., Mouhri, A., Labarthe, B., Biancamaria, S., Rivière, A., Weill, P., 2014. Continental hydrosystem modelling: the concept of nested stream-aquifer interfaces. *Hydrol. Earth Syst. Sci.* 18, 3121–3149.
- Foster, S.B., Allen, D.M., 2015. Groundwater-surface water interactions in a mountain-to-coast watershed: effects of climate change and human stressors. *Adv. Meteorol.* Article ID 861805.
- Garambois, P., Monnier, J., 2015. Inference of effective river properties from remotely sensed observations of water surface. *Adv. Water Resour.* 79, 103–120.
- Graham, P.W., Andersen, M.S., McCabe, M.F., Ajami, H., Baker, A., Acworth, I., 2015. To what extent do long-duration high-volume dam releases influence river-aquifer interactions? A case study in New South Wales, Australia. *Hydrogeol. J.* 23, 319–334.
- IGN, 2015. BD ALTI Version 2.0. Tech. Rep. Institut Géographique National.
- Käser, D., Binley, A., Heathwaite, A., 2013. On the importance of considering channel microforms in groundwater models of hyporheic exchange. *River Res. Appl.* 29, 528–535.
- Käser, D., Graf, T., Cochand, F., McLaren, R., Therrien, R., Brunner, P., 2014. Channel representation in physically based models coupling groundwater and surface water: pitfalls and how to avoid them. *Ground Water* 52 (6), 827–836.
- King, D., Bas, C.L., Jamagne, M., et J. Daroussin, H., 1995. Base de données géographique des sols de France à l'échelle du 1/1,000,000. Notice générale d'utilisation. Tech. Rep. Service d'étude des sols et de la carte pédologique (INRA).
- Knight, J., Rassam, D., 2007. Groundwater head responses due to random stream stage fluctuations using basis splines. *Water Resour. Res.* 43, W06501.
- Kurtulus, B., Flipo, N., Goblet, P., Vilain, G., Tournébeize, J., Tallec, G., 2011. Hydraulic head interpolation in an aquifer unit using ANFIS and ordinary kriging. *Studies in Computational Intelligence*, vol. 343. Springer, pp. 265–273.
- Lalot, E., Curie, F., Wawrzyniak, V., Baratelli, F., Schomburgk, S., Flipo, N., Piegay, H., Moatar, F., 2015. Quantification of the contribution of the Beauce groundwater aquifer to the discharge of the Loire River using thermal infrared satellite imaging. *Hydrol. Earth Syst. Sci.* 19, 4479–4492.
- Latapie, A., Camenen, B., Rodrigues, S., Paquier, A., Bouchard, J.P., Moatar, F., 2014. Assessing channel response of a long river influenced by human disturbance. *Catena* 121, 1–12.
- Leblais, E., 2008. Hydro-Logical Processing of Geographical Information - Part One: DEM, Drainage Pattern, Rivers, Basins. Tech. Rep. Cemagref, Lyon, France, 44p.
- Ledoux, E., 1975. Programme NEWSAM: principe et notice d'emploi Tech. Rep. Centre d'Informatique Géologique, Ecole Nationale Supérieure des Mines de Paris.
- Levassor, A., Ledoux, E., 1996. Programme NEWSAM - Notice d'utilisation Tech. Rep. Centre d'Informatique Géologique, Ecole Nationale Supérieure des Mines de Paris.
- Massei, N., Laignel, B., Deloffre, J., Mesquita, J., Motelay, A., Lafite, R., Durand, A., 2010. Long-term hydrological changes of the Seine River flow (France) and their relation to the North Atlantic Oscillation over the period 1950–2008. *Int. J. Climatol.* 30 (14), 2146–2154.
- McGuire, K., McDonnell, J., Weiler, M., Kendall, C., McGlynn, B., Welker, J., Seibert, J., 2005. The role of topography on catchment-scale water residence time. *Water Resour. Res.* 41, W05002.
- Mejia, A., Reed, S., 2011. Role of channel and floodplain cross-section geometry in the basin response. *Water Resour. Res.* 47, W09518.
- Moatar, F., Gailhard, J., 2006. Water temperature behaviour in the River Loire since 1976 and 1881. *C.R. Geosci.* 338, 319–328.
- Monteil, C., 2011. Estimation de la contribution des principaux aquifères du bassin-versant de la Loire au fonctionnement hydrologique du fleuve à l'étiage Ph.D. thesis. MINES-ParisTech, 60 bd Saint Michel, Paris.
- Nash, J., Sutcliffe, J., 1970. River flow forecasting through conceptual models. Part I. A discussion of principles. *J. Hydrol.* 10, 282–290.
- Pasquier, P., Marcotte, D., 2006. Steady- and transient-state inversion in hydrogeology by successive flux estimation. *Adv. Water Resour.* 29 (12), 1934–1952.
- Pavelsky, T., Smith, L., 2008. RivWidth: a software tool for the calculation of river widths from remotely sensed imagery. *IEEE Geosci. Remote Sens. Lett.* 5 (1), 70–73.
- Ponzini, G., Lozej, A., 1982. Identification of aquifer transmissivities: the comparison model method. *Water Resour. Res.* 18 (3), 597–622.
- Pryet, A., Labarthe, B., Saleh, F., Akopian, M., Flipo, N., 2015. Reporting of stream-aquifer flow distribution at the regional scale with a distributed process-based model. *Water Resour. Manage.* 29, 139–159.
- Quintana-Seguí, P., Moigne, P.L., Durand, Y., Martin, E., Habets, F., Baillon, M., Canellas, C., Franchisteguy, L., Morel, S., 2008. Analysis of near-surface atmospheric variables: validation of the SAFRAN analysis over France. *J. Appl. Meteorol. Climatol.* 47, 92–107.
- Rivière, A., Gonçalves, J., Jost, A., Font, M., 2014. Experimental and numerical assessment of transient stream-aquifer exchange during disconnection. *J. Hydrol.* 517, 574–583.
- Rosenberry, D., Sheibley, R., Cox, S., Simonds, F., Naftz, D., 2013. Temporal variability of exchange between groundwater and surface water based on high-frequency direct measurements of seepage at the sediment-water interface. *Water Resour. Res.* 49, 2975–2986.
- Rushton, K., 2007. Representation in regional models of saturated river-aquifer interaction for gaining/losing rivers. *J. Hydrol.* 334, 262–281.
- Rushton, K., Tomlinson, L., 1979. Possible mechanisms for leakage between aquifers and rivers. *J. Hydrol.* 40, 49–65.
- Saleh, F., 2010. Apport de la modélisation hydraulique pour une meilleure simulation des tirants d'eau et des échanges nappe-rivière à l'échelle régionale Ph.D. thesis. Université Pierre et Marie Curie.
- Saleh, F., Ducharme, A., Flipo, N., Oudin, L., Ledoux, E., 2013. Impact of river bed morphology on discharge and water levels simulated by a 1d saint-venant hydraulic model at regional scale. *J. Hydrol.* 476, 169–177.
- Saleh, F., Flipo, N., Habets, F., Ducharme, A., Oudin, L., Vennot, P., Ledoux, E., 2011. Modeling the impact of in-stream water level fluctuations on stream-aquifer interactions at the regional scale. *J. Hydrol.* 400 (3–4), 490–500.
- Scibek, J., Allen, D., Cannon, A., Whitfield, P., 2007. Groundwater-surface water interaction under scenarios of climate change using a high-resolution transient groundwater model. *J. Hydrol.* 333, 165–181.
- Scibek, J., Allen, D.M., 2006. Comparing modelled responses of two high-permeability, unconfined aquifers to predicted climate change. *Global Planet. Change* 50, 50–62.
- Shope, C., Constantz, J., Cooper, C., Reeves, D., Pohl, G., McKay, W., 2012. Influence of a large fluvial island, streambed, and stream bank on surface water-groundwater fluxes and water table dynamics. *Water Resour. Res.* 48, W06512.
- Soille, P., 2004. Optimal removal of spurious pits in grid digital elevation models. *Water Resour. Res.* 40, W12509. <http://dx.doi.org/10.1029/2004WR003060>.
- Strahler, A., 1957. Quantitative analysis of watershed geomorphology. *Geophys. Union Trans.* 38, 913–920.
- Trauth, N., Schmidt, C., Vieweg, M., Oswald, S., Fleckenstein, J., 2015. Hydraulic controls of in-stream gravel bar hyporheic exchange and reactions. *Water Resour. Res.* 51, 2243–2263.
- Valette, L., Cunillera, A., 2010. Cahiers techniques SYRAH-CE Tech. Rep. Pole Hydroécologie des cours d'eau Onema Cemagref Lyon.
- Waibel, M.S., Gannett, M.W., Chang, H., Hulbe, C.L., 2013. Spatial variability of the response to climate change in regional groundwater systems - examples from simulations in the Deschutes Basin, Oregon. *J. Hydrol.* 486, 187–201.
- Wörman, A., Packman, A., Marklund, L., Harvey, J., Stone, S., 2007. Fractal topography and subsurface water flows from fluvial bedforms to the continental shield. *Geophys. Res. Lett.* 34, L07402.
- Xie, Y., Cook, P.G., Brunner, P., Irvine, D.J., Simmons, C.T., 2014. When can inverted water tables occur beneath streams? *Ground Water* 52 (5), 769–774.
- Yamazaki, D., Baugh, C.A., Bates, P.D., Kanae, S., Alsdorf, D.E., Oki, T., 2012. Adjustment of a spaceborne DEM for use in floodplain hydrodynamic modeling. *J. Hydrol.* 436–437, 81–91.

- Yamazaki, D., Loughlin, F.O., Trigg, M., Miller, Z., Pavelsky, T., Bates, P., 2014. Development of the global width database for large rivers. *Water Resour. Res.* 50, 3467–3480.
- Zachara, J.M., Long, P.E., Bargar, J., Davis, J.A., Fox, P., Fredrickson, J.K., Freshley, M.D., Konopka, A.E., Liu, C., McKinley, J.P., Rockhold, M.L., Williams, K.H., Yabusaki, S. B., 2013. Persistence of uranium groundwater plumes: contrasting mechanisms at two DOE sites in the groundwater–river interaction zone. *J. Contam. Hydrol.* 147, 45–72.
- Zume, J., Tarhule, A., 2008. Simulating the impacts of groundwater pumping on stream–aquifer dynamics in semiarid northwestern Oklahoma, USA. *Hydrogeol. J.* 16, 797–810.
- Zume, J., Tarhule, A., 2011. Modelling the response of an alluvial aquifer to anthropogenic and recharge stresses in the United States Southern Great Plains. *J. Earth Syst. Sci.* 4, 557–572.